

# Tsunami earthquakes: the quest for a regional signal

Emile A. Okal\*, Andrew V. Newman<sup>1</sup>

*Department of Geological Sciences, Northwestern University,  
Evanston, IL 60201, USA*

Received 24 July 2000; accepted 29 January 2001

## Abstract

Using the technique developed by Newman and Okal [J. Geophys. Res. 103 (1998) 26885], a dataset of digital records from 84 earthquakes is analyzed to investigate their source slowness in the quest for a possible regional signal in three subduction zones which experienced recent tsunami earthquakes (Nicaragua, 1992; Java, 1994; Peru, 1996). The dataset is augmented by analog seismograms from historical events, including major tsunamigenic earthquakes of the past 65 years. We fail to detect a regional trend for slowness, which suggests that the latter may be controlled on a more local scale by morphological structures of the subducting plate. No correlation is found between slowness and either depth, focal mechanism, or seismic moment. In Nicaragua, we document two slow historical earthquakes located on the slab down-dip from the 1992 shock. The most interesting results are in Peru, where a local area of slowness is tentatively defined around the source of the 1960 tsunami earthquake, and where both the 1996 and 1960 tsunami earthquakes occur at the intersection of the trench with major topographic features on the Nazca plate, the Mendaña fracture zone and the Trujillo trough, respectively. © 2001 Elsevier Science B.V. All rights reserved.

*Keywords:* Slow earthquakes; Tsunamis; Subduction zones

## 1. Introduction

For close to 30 years now, seismologists have been intrigued by the so-called ‘tsunami earthquakes’, whose tsunamis have greater amplitudes than would be expected from their seismic waves. Kanamori (1972) described in those terms the 1896 Sanriku and 1946 Aleutian events. Later, Fukao (1979) identified the main aftershock (20th October) of the 1963 Kuriles earthquake and the 1975 Kuriles event as tsunami earthquakes. In the past decade, three events

qualified as tsunami earthquakes: the 1992 Nicaragua, 1994 Java, and 1996 Chimbote, Peru, events.

Tsunami earthquakes are of particular concern in the context of warning, and more generally mitigation, because their low seismic magnitudes can occasionally result in their not being felt by the population who, as a result, may not take precautionary evasive measures such as the immediate evacuation of beaches and low-lying areas.

Two fundamental models have been proposed to explain the disparity between seismic and tsunami wave excitation during tsunami earthquakes.

- The first model involves the concept of a slower than usual source rupture, resulting in destructive interference at the higher frequencies used in conventional magnitudes. The latter then underestimate

\* Corresponding author. Tel.: +1-847-491-3238;  
fax: +1-847-491-8060.

E-mail address: emile@earth.nwu.edu (E.A. Okal).

<sup>1</sup> Present address: Earth Sciences Board, University of California, Santa Cruz, CA 95064, USA.

the true size of the earthquake, while the amplitude of the tsunami waves is controlled by the very low-frequency components of the source, for which the interference remains constructive. Examples include the 1963 (20th October) and 1975 Kuriles events, as well as the 1992 Nicaragua, 1994 Java, and 1996 Peru (Chimbote) shocks.

- The second class of earthquakes with enhanced tsunami excitation involves an underwater landslide or slump, triggered by the earthquake, in a coseismic or slightly delayed mode. Examples are the 1929 Grand Banks and 1998 Papua New Guinea events (Hasegawa and Kanamori, 1987; Okal, 1999; Synolakis et al., 2001). Such events are generally not referred to as ‘tsunami earthquakes’, and will not be considered further in the present paper. The case of the 1946 Aleutian earthquake, which unleashed the largest transpacific tsunami of the past century, remains presently unresolved (Kanamori, 1985; Okal, 1992; Pelayo and Wiens, 1992; Johnson and Satake, 1997; Fryer and Watts, 2000).

The origin of the slow rupture responsible for tsunami earthquakes has been attributed usually to the presence of sedimentary material involved in the subduction process and featuring weak mechanical properties. Several scenarios have been proposed in this respect.

- In heavily sedimented areas, i.e. in the case of the subduction of older oceanic lithosphere, the development of an accretionary prism provides a volume of material with weak mechanical properties, leading to a slower source regime when rupture propagates through that structure. In the Kuriles, Fukao (1979) has proposed as a mechanism for the 1963 and 1975 tsunami earthquakes their triggering by stress transfer into the accretionary prism, following the 1963 mainshock (13th October), and the 1973 Nemuro-Oki event, respectively. In areas with relatively weaker coupling, it has also been proposed that the subduction of sediment may ‘lubricate’ the fault to the extent that the rupture velocity decreases sharply, thus giving the source an anomalously long duration (Satake and Tanioka, 1999).

However, the mechanism proposed by Fukao (1979) for the Kuriles cannot be applied to the 1992, 1994 and 1996 events, since detailed studies

of their ruptures has revealed that all three took place at the respective plate interfaces (Tanioka and Satake, 1996; Ihmlé, 1996; Ihmlé et al., 1998; Felzer et al., 1999; Polet and Kanamori, 2000).

- As noted by Byrne et al. (1988), the shallowest part of the subduction interface may not be rupturing seismically, but rather the site of continuous creep, under the influence of a sedimentary layer at the subduction interface. However, in a recent model, Tanioka et al. (1997) have proposed that, in a sediment-starved environment, the lack of subducted sediment may lead to an upward extension of the seismogenic zone and, in the presence of ridge-and-graben structures, to a jerky and hence slow rupture. It is noteworthy that the three tsunami earthquakes of 1992, 1994 and 1996 featured upwards propagation along the plate interface (Kikuchi and Kanamori, 1995; Ihmlé, 1996; Ihmlé et al., 1998; Polet and Kanamori, 2000); however, the Ihmlé’s (1996) source slip inversion of the 1992 Nicaraguan earthquake suggests a slow but smooth propagation of the rupture. The model of Tanioka et al. (1997) was later expanded by Polet and Kanamori (2000).

In this or any other context seeking to model the slowness of a tsunami earthquake as due to an anomalous structural property of the seismic interface, the question then arises of the possible regional character of any such anomaly. In other words, do all earthquakes in a subduction province such as Nicaragua with one documented slow ‘tsunami earthquake’, share this character of source slowness? Should the answer be affirmative, one would expect future earthquakes in the same region to also feature a slow source. Such a region would then possess a particularly enhanced form of tsunami risk, and special efforts would be warranted in terms of both real-time detection of slow earthquakes, and specific education of the populations at risk.

The subject of this paper is to conduct a systematic survey of the level of source slowness in earthquakes occurring in the three subduction systems (central America, Sunda, Peru) which experienced tsunami earthquakes during the 1990s. Of particular interest in the quest for a regional signal are the following questions which will guide us in the three study areas of the present paper.

- Are aftershocks of a slow ‘tsunami earthquake’, which are expected to take place on the same fault segment, themselves equally slow?
- Along segments of a subduction zone neighboring the fault zone of a ‘tsunami earthquake’, do other tsunamigenic events feature source slowness?
- What can be learned from the historical, pre-digital seismic record?

## 2. Methodology

In a previous paper (Newman and Okal, 1998; hereafter Paper I), we adapted Boatwright and Choy’s (1986) computation of the energy radiated by a seismic source to the real-time situation when neither source depth nor focal mechanism is known accurately. In particular, this approach, which uses the philosophy of a magnitude scale, avoids the systematic over-estimation of energy in the case of strike-slip earthquakes, which was due to the inability of Boatwright and Choy’s algorithm to account for small scale lateral heterogeneity at the source.

We defined in Paper I a discriminant,  $\Theta = \log_{10} E^E/M_0$  (where  $E^E$  is the estimated energy, and  $M_0$  the seismic moment), and showed that  $\Theta$  efficiently segregates slow events and in particular tsunami earthquakes. Of a dataset of 52 earthquakes studied in Paper I, only four had  $\Theta$  less than  $-5.7$ : the three tsunami earthquakes of the 1990s (1992 Nicaragua:  $\Theta = -6.30$ ; 1994 Java:  $\Theta = -6.01$ ; 1996 Chimbote, Peru:  $\Theta = -5.94$ ), as well as the smaller 1982 Tonga earthquake ( $\Theta = -5.76$ ), which was described by Talandier and Okal (1989) as a ‘tsunami earthquake’, on account of the amplitude of its tsunami at Papeete.

In the present study, we apply the formalism of Paper I to regional datasets of earthquakes in the central American, Sunda, and Peruvian subduction zones. Against the average value  $\Theta_{av} = -4.90$  predicted theoretically in Paper I from scaling laws, we use  $\Theta = -5.7$  as the threshold characterizing an earthquake as ‘slow’. In a direct extension of Paper I, we initially targeted for study all events in the years 1980–1997 with Harvard CMT moments greater than  $10^{25}$  dyn cm (Dziewonski et al., 1987 and subsequent quarterly updates). The large Indonesian event of 19 August 1977 was also included.

### 2.1. Historical events

The method developed in Paper I relies on the availability of digital data, sampled at a rate of at least 10 Hz, in order to carry out Boatwright and Choy’s (1986) energy integral to the standard upper frequency bound of 2 Hz defined in Paper I. This has limited

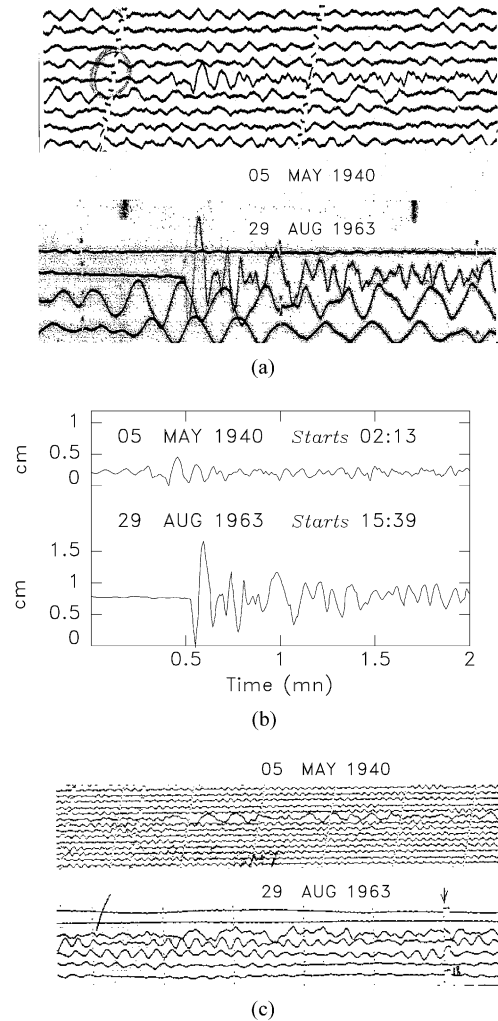


Fig. 1. (a) Vertical Benioff 1–90 records at Pasadena of  $P$  waves from the Peruvian earthquakes of 5 May 1940 (top) and 29 August 1963 (bottom). Despite similar long-period moments, the events show a spectacular difference in the high-frequency content of their  $P$  waves. (b) Plot of the digitized time series from which the estimated energy was computed. (c) Close-up of the Rayleigh-wave windows of the two seismograms; note that the difference in amplitudes is much less pronounced. The aspect ratio of the original seismograms is common to all traces in all frames.

Table 1  
Digital dataset

Date (D M (J) Y)	Epicenter		Depth (km)	Seismic moment $M_0$ ( $10^{27}$ dyn cm)	Estimated energy $E^E$ ( $10^{21}$ erg)	$\Theta$	No. of stations	Variance
	$^{\circ}$ N	$^{\circ}$ E						
Central America								
17 August (229) 1981	14.52	-93.77	23	0.013	0.044	-5.47	2	0.13
12 January (012) 1982	12.80	-87.30	10	0.018	0.113	-5.20	5	0.41
6 April (096) 1982	13.79	-91.95	64	0.140	0.567	-5.39	6	0.43
19 June (170) 1982	12.65	-88.97	70	1.050	3.154	-5.52	4	0.20
3 April (093) 1983	8.85	-83.25	44	1.800	7.038	-5.41	10	0.44
9 May (129) 1983	8.06	-82.87	39	0.029	0.186	-5.19	4	0.19
3 July (184) 1983	9.65	-83.26	12	0.038	0.091	-5.62	6	0.67
18 July (199) 1983	12.51	-87.22	91	0.055	0.390	-5.15	5	0.24
12 October (285) 1983	7.96	-82.53	34	0.011	0.029	-5.59	7	0.54
2 December (336) 1983	13.86	-92.20	68	0.370	1.698	-5.34	5	0.59
10 December (344) 1983	14.32	-91.73	86	0.012	0.069	-5.24	4	0.52
20 December (355) 1984	11.39	-86.34	71	0.010	0.105	-4.98	4	0.25
19 April (109) 1985	11.46	-87.42	84	0.018	0.243	-4.87	4	0.28
3 June (154) 1985	13.14	-90.19	51	0.028	0.124	-5.35	4	0.38
16 December (350) 1985	11.65	-85.58	31	0.016	0.057	-5.45	7	0.44
12 March (071) 1987	15.61	-94.39	38	0.015	0.045	-5.52	4	0.19
8 April (098) 1987	11.62	-86.46	65	0.050	0.140	-5.55	6	0.35
4 October (277) 1987	10.80	-85.94	52	0.020	0.163	-5.09	5	0.46
17 November (321) 1987	12.49	-87.07	92	0.058	0.407	-5.15	3	0.16
11 March (071) 1988	9.12	-82.96	23	0.013	0.023	-5.74	4	0.31
3 November (308) 1988	13.84	-90.61	70	0.090	0.868	-5.02	6	0.56
25 March (084) 1990	9.95	-84.78	22	1.100	7.831	-5.15	8	0.44
3 April (093) 1990	11.42	-86.32	56	0.180	0.998	-5.26	9	0.33
28 April (118) 1990	8.95	-83.48	30	0.042	1.216	-4.54	10	0.42
22 December (356) 1990	9.95	-84.24	20	0.010	0.032	-5.50	5	0.21
16 March (075) 1991	10.13	-85.24	59	0.032	0.325	-4.99	8	0.20
22 April (112) 1991	9.70	-83.08	4	3.300	10.237	-5.51	7	0.29
24 April (114) 1991	9.79	-83.56	13	0.018	0.064	-5.45	7	0.46
4 May (124) 1991	9.57	-82.42	10	0.021	0.074	-5.45	7	0.32
18 September (261) 1991	14.58	-91.04	11	0.022	0.058	-5.58	7	0.25
7 March (067) 1992	10.23	-84.31	74	0.065	0.958	-4.83	9	0.39
18 May (139) 1992	7.40	-82.33	18	0.033	0.698	-4.67	10	0.43
23 May (144) 1992	13.45	-90.03	80	0.011	0.056	-5.29	5	0.34
30 May (151) 1992	14.44	-92.95	53	0.035	0.129	-5.44	9	0.23
2 September (246) 1992	11.20	-87.81	21	3.400	1.709	-6.30	11	0.07
2 September (246) 1992 (b)	11.26	-86.74	42	0.013	0.052	-5.40	9	0.19
5 September (249) 1992	12.04	-87.39	63	0.011	0.088	-5.10	8	0.23
28 September (272) 1992	13.43	-90.73	70	0.012	0.169	-4.85	7	0.24
3 September (246) 1993	14.57	-92.81	66	0.150	1.153	-5.11	16	0.36
10 September (253) 1993 (a)	14.41	-92.79	61	0.013	0.058	-5.35	5	0.34
10 September (253) 1993 (b)	14.74	-92.69	36	0.830	12.844	-4.81	11	0.21
12 September (255) 1993	13.90	-90.50	56	0.011	0.099	-5.05	8	0.40
19 September (262) 1993	14.44	-93.31	36	0.049	0.318	-5.19	16	0.34
30 September (273) 1993	15.18	-94.86	30	0.060	0.469	-5.11	13	0.38
15 March (074) 1994	11.16	-88.08	23	0.014	0.127	-5.04	8	0.57
14 June (165) 1995	12.15	-88.36	36	0.075	1.040	-4.86	15	0.31
14 September (257) 1995	16.88	-98.60	44	1.300	24.806	-4.72	9	0.29
4 September (248) 1996	9.37	-84.36	35	0.022	0.107	-5.31	18	0.33
1 April (091) 1997	7.78	-82.39	31	0.016	0.101	-5.19	7	0.40
19 July (200) 1997	16.34	-98.19	31	0.119	0.677	-5.25	7	0.12

Table 1 (Continued)

Date (D M (J) Y)	Epicenter		Depth (km)	Seismic moment $M_0$ ( $10^{27}$ dyn cm)	Estimated energy $E^E$ ( $10^{21}$ erg)	$\Theta$	No. of stations	Variance
	$^{\circ}$ N	$^{\circ}$ E						
Java								
19 August (231) 1977	−11.14	118.23	53	36.000	398.000	−4.96	1	0.00
11 March (070) 1982	−9.35	118.30	33	0.074	2.995	−4.39	4	0.22
7 August (219) 1982	−11.18	115.45	55	0.056	1.706	−4.52	6	0.44
4 October (278) 1984	−10.04	119.12	36	0.037	0.434	−4.93	5	0.34
22 March (081) 1985	−7.00	105.05	45	0.040	0.207	−5.29	6	0.35
19 December (353) 1986	−10.91	119.81	25	0.043	0.197	−5.34	4	0.16
17 December (351) 1987	−9.44	114.47	46	0.012	0.170	−4.84	5	0.37
17 August (230) 1988	−7.58	107.80	27	0.012	0.287	−4.62	6	1.39
5 July (186) 1991	−9.65	114.60	37	0.016	0.185	−4.94	8	0.41
12 December (347) 1992	−8.34	122.49	28	5.100	122.841	−4.62	6	0.32
2 June (153) 1994	−11.03	113.04	18	5.300	4.895	−6.03	12	0.40
3 June (154) 1994	−10.75	113.14	26	0.088	3.247	−4.43	12	0.10
4 June (155) 1994	−10.94	113.52	11	0.058	2.633	−4.34	13	0.27
5 June (156) 1994	−10.27	113.60	26	0.014	1.792	−3.89	10	0.48
15 June (166) 1994 (a)	−10.43	113.75	35	0.014	0.632	−4.35	10	0.47
15 June (166) 1994 (b)	−10.31	113.69	29	0.015	0.361	−4.62	8	0.28
12 February (043) 1996	−11.23	118.93	43	0.015	0.244	−4.79	21	0.37
9 December (344) 1996	−8.32	107.44	55	0.014	0.159	−4.94	21	0.53
17 March (076) 1997	−7.27	105.41	51	0.042	0.555	−4.88	17	0.30
Peru								
7 March (067) 1980	−17.17	−73.48	53	0.019	0.046	−5.61	2	0.28
28 February (059) 1981	−6.72	−82.17	22	0.015	0.045	−5.52	3	0.04
19 November (323) 1982	−10.44	−74.95	14	0.106	3.058	−4.54	3	0.43
21 August (233) 1985	−8.90	−78.82	45	0.041	0.643	−4.80	4	0.55
12 April (103) 1988	−17.55	−72.83	33	0.480	2.659	−5.26	5	0.38
13 April (104) 1988	−17.66	−73.21	16	0.022	0.409	−4.73	5	0.53
20 March (079) 1991	−5.94	−80.94	43	0.011	0.039	−5.45	3	0.45
21 March (080) 1991	−9.78	−80.07	25	0.019	0.088	−5.33	5	0.06
5 April (095) 1991	−14.20	−75.61	49	0.030	0.491	−4.79	4	0.64
1 July (182) 1991	−15.88	−75.01	33	0.011	0.034	−5.51	6	0.10
16 May (137) 1992	−13.52	−76.73	52	0.014	0.063	−5.34	5	0.08
21 February (052) 1996	−9.95	−80.23	10	2.200	2.216	−6.00	11	0.34
12 November (317) 1996	−15.04	−75.37	33	4.400	43.579	−5.00	8	0.17
13 November (318) 1996	−14.86	−75.97	35	0.014	0.059	−5.36	9	0.22
9 February (040) 1997	−14.41	−76.42	10	0.017	0.162	−5.02	14	0.26

our previous work to events post-dating the development of digital instrumentation, in practice 1975. Because of the relative rarity of large tsunamigenic earthquakes, it is desirable to apply the same technique to historical events. We have found it possible to use records obtained on Benioff ‘1–90’ instruments (Benioff, 1955), which can be regarded as ancestors to the modern broad-band seismometers and hence have an appropriate response in the whole range of integration (0.1–2 Hz). We obtain a high fidelity of digitized output with a sampling  $\delta t = 0.1$  s, by simply hand-digitizing the records following optical magni-

fication, by a typical factor of eight. This procedure is illustrated on Fig. 1, which compares 1–90 records obtained for a slow earthquake and a regular one. In the present study, we apply this technique to a number of key events, such as the 1950 Costa Rica and 1940 Peru earthquakes. The operation of the 1–90 system at Caltech was discontinued in February 1992, but we were able to simulate a 1–90 record of the 1992 Nicaragua earthquake from the Terrascope Pasadena record. We then processed the simulated record, finding  $\Theta = -6.21$ , in excellent agreement with other determinations for this event (see Paper I), thus



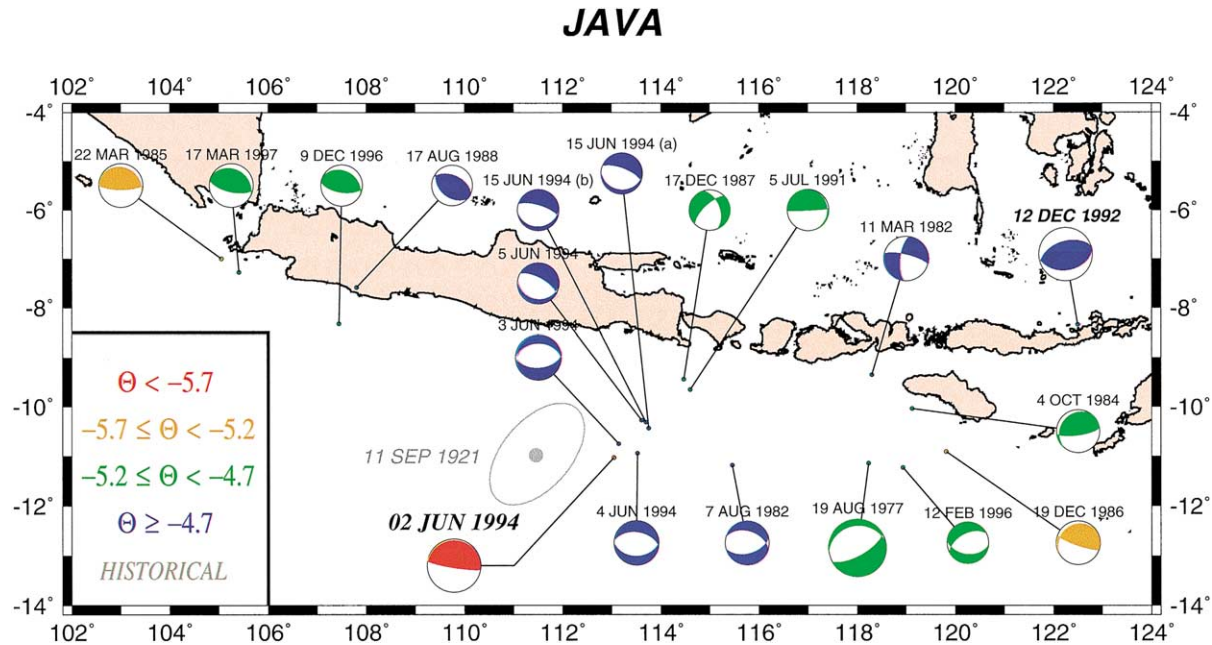


Fig. 3. Same as figure 2 for Java.

Before presenting a discussion of our results in the tectonic context of each of the three regions investigated, we eliminate the possibility that source slowness could be an artifact of hypocentral depth or focal mechanism, or that it may correlate significantly with moment.

### 3.1. Correlation with depth

We first investigate any possible correlation between source depth and slowness. We are motivated by the speculation that, if slowness is associated in some way with the presence of sedimentary phases at the interface, it should be confined to the particular depth range where these phases are thermodynamically expected. In addition, events taking place outside the plate interface, i.e. inside the slab or in the overlying wedge, would be unaffected.

Fig. 5 plots slowness versus depth for each of the three subduction zones studied. It shows that no correlation between  $\Theta$  and depth  $d$  can be resolved. The best-fitting regressions, showed as the dashed line on each frame, are found to be  $\Theta = 4.13 \times 10^{-3}d - 5.43$  in central America,  $\Theta = -2.71 \times 10^{-3}d - 4.68$  in Java,

and  $\Theta = 1.94 \times 10^{-3}d - 5.25$  in Peru ( $d$  in km). Note in particular the slopes of opposite signs in central America and Java. In addition, these regressions are of poor quality, as documented by the mediocre correlation coefficients:  $-0.08$  in Java,  $0.08$  in Peru, and no more than  $0.32$  in central America. In the latter region, the tentative trend of  $\Theta$  with depth could not account for the extreme slowness of the 1992 Nicaragua event, even if it were displaced all the way to the surface. We conclude that  $\Theta$  is not related to depth in any of the three subduction zones studied.

We note, however, that the depths used in this figure are ISC hypocentral depths. Significant differences exist occasionally with depths computed by the NEIC or other agencies, and with centroid depths inverted into the Harvard catalogue. In this respect, the accuracy of these depth estimates may be less than their reported precision.

### 3.2. Correlation with focal mechanism

Next, we explore the possibility that slowness could correlate with the geometry of the source. Different focal mechanisms obviously express the release of

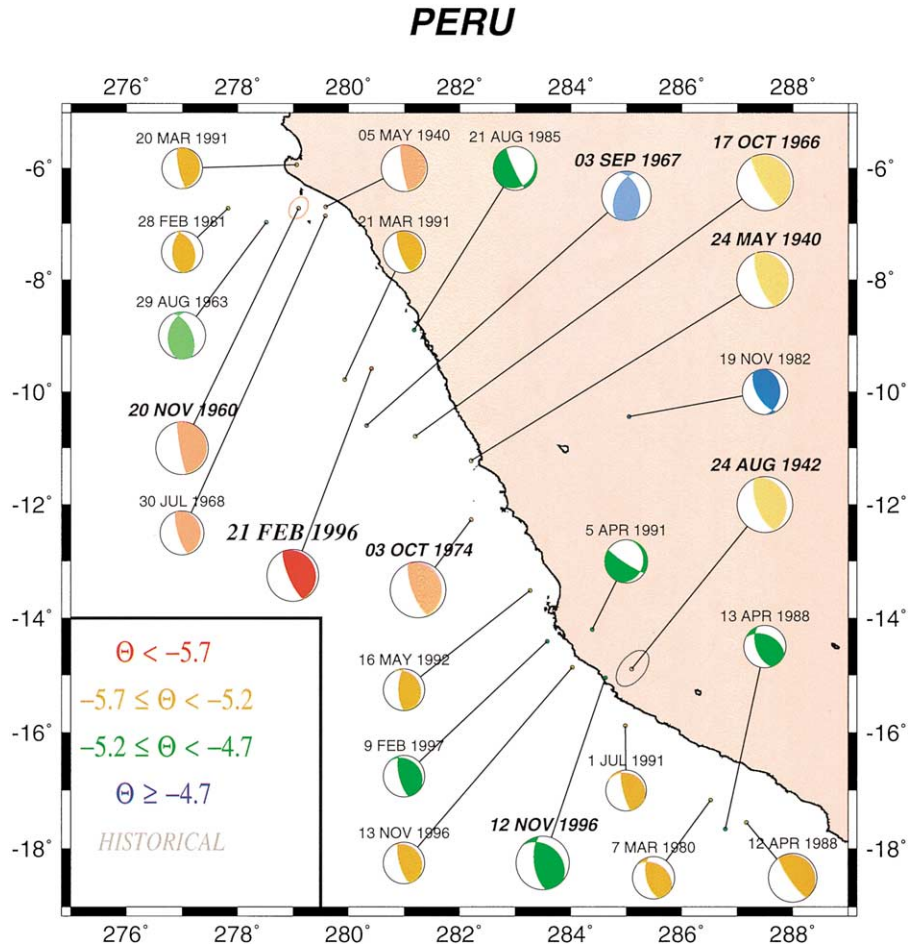


Fig. 4. Same as figure 2 for Peru.

different stresses, which could be taking place in different geometrical environments (e.g. intraplate versus interplate), involving materials with different mineralogies, and hence different mechanical properties. On the three frames of Fig. 6, we have plotted the focal mechanisms of the events in our dataset in the triangular representation of Frohlich and Apperson (1992). This method describes a double-couple mechanism in terms of the dip angles of its compressional ( $P$ ), tensional ( $T$ ) and null ( $N$ ) principal axes, with the end-member geometries, strike-slip ( $N$  vertical), 45°-dipping thrust fault ( $T$  vertical) and 45°-dipping normal fault ( $P$  vertical), plotted at the vertices of an equilateral triangle. No obvious correlation between  $\theta$  and focal mechanism is apparent on Fig. 6,

but in order to quantify this assertion, we define a correlation vector  $\mathbf{r}$  as

$$\mathbf{r} = \frac{\sum_{i=1}^N (\theta_i - \bar{\theta})(\mathbf{x}_i - \bar{\mathbf{x}})}{\left[ \sum_{i=1}^N (\theta_i - \bar{\theta})^2 \right]^{1/2} \left[ \sum_{i=1}^N (\mathbf{x}_i - \bar{\mathbf{x}})^2 \right]^{1/2}} \quad (1)$$

where and for each point  $i$  in the dataset, the vector  $\mathbf{x}_i$  is the cartesian representation of the focal mechanism given in Eqs. (14) of Frohlich and Apperson (1992), and the overscore indicates a mean value (note a typographic error in the denominator of these authors' equations, which in both instances should read  $(\sin(35.26^\circ) \sin \delta_B + \cos(35.26^\circ) \cos \delta_B \cos \psi$ ; Frohlich, personal communication, 2000)). For a given population of earthquakes, the correlation vector

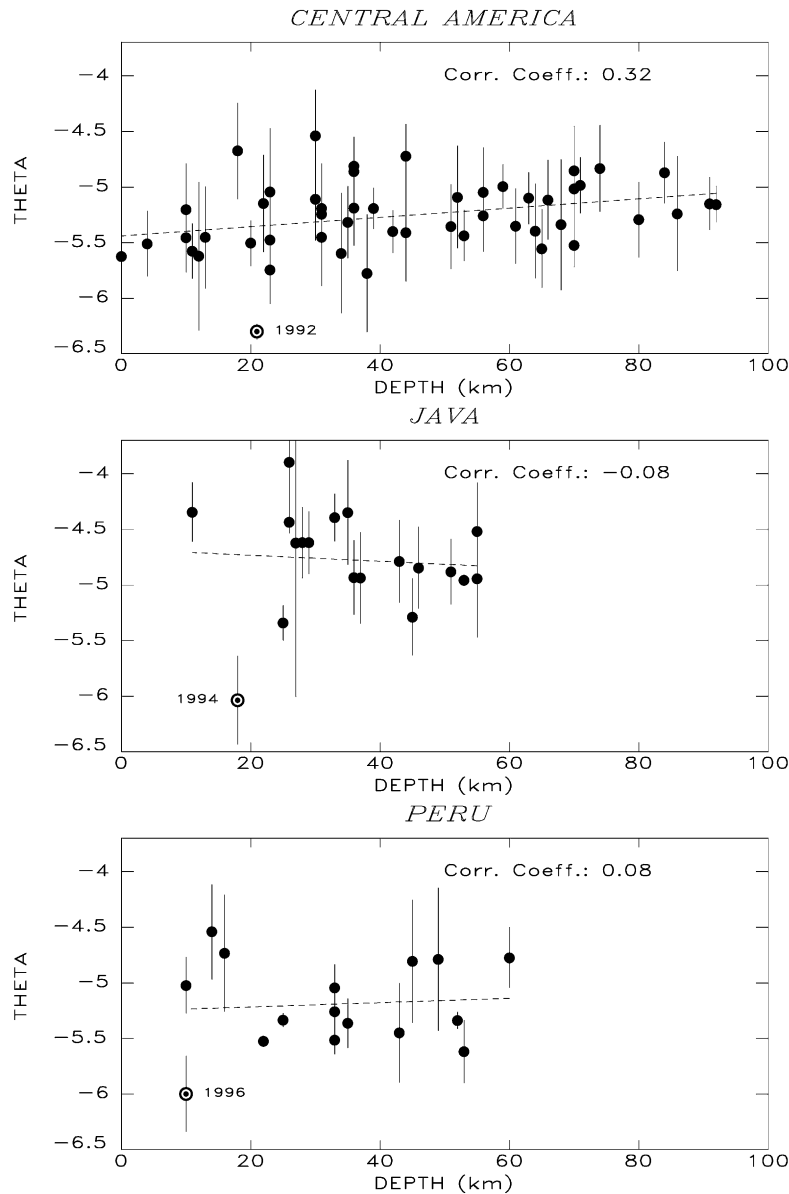


Fig. 5. Slowness parameter  $\theta$  vs. depth for the digital dataset. Bull's eye symbols identify the three tsunami earthquakes. For each event, the error bar expresses the scatter of  $\theta$  computed at individual stations (the bar would be smaller than the size of the symbol for the 1992 tsunami earthquake in Nicaragua). Dashed lines are best-fitting regressions, with correlation coefficients also given.

$\mathbf{r}$  can be interpreted as follows. Its modulus,  $r$ , is a measure of the degree of correlation of  $\theta$  with the two-dimensional variable  $\mathbf{x}$ ; it would be 1, if  $\theta$  were a linear combination of the components  $h$  and  $v$  of the vector  $\mathbf{x}$  (in the notation of Frohlich and Apperson

(1992)). The direction of the vector  $\mathbf{r}$  is related to that of the best-fitting gradient of  $\theta$  in the plane. We find mediocre levels of correlation for the central American dataset ( $r = 0.16$ ) and in Peru ( $r = 0.13$ ). In Java, the correlation rises to  $r = 0.35$ , with  $\mathbf{r}$

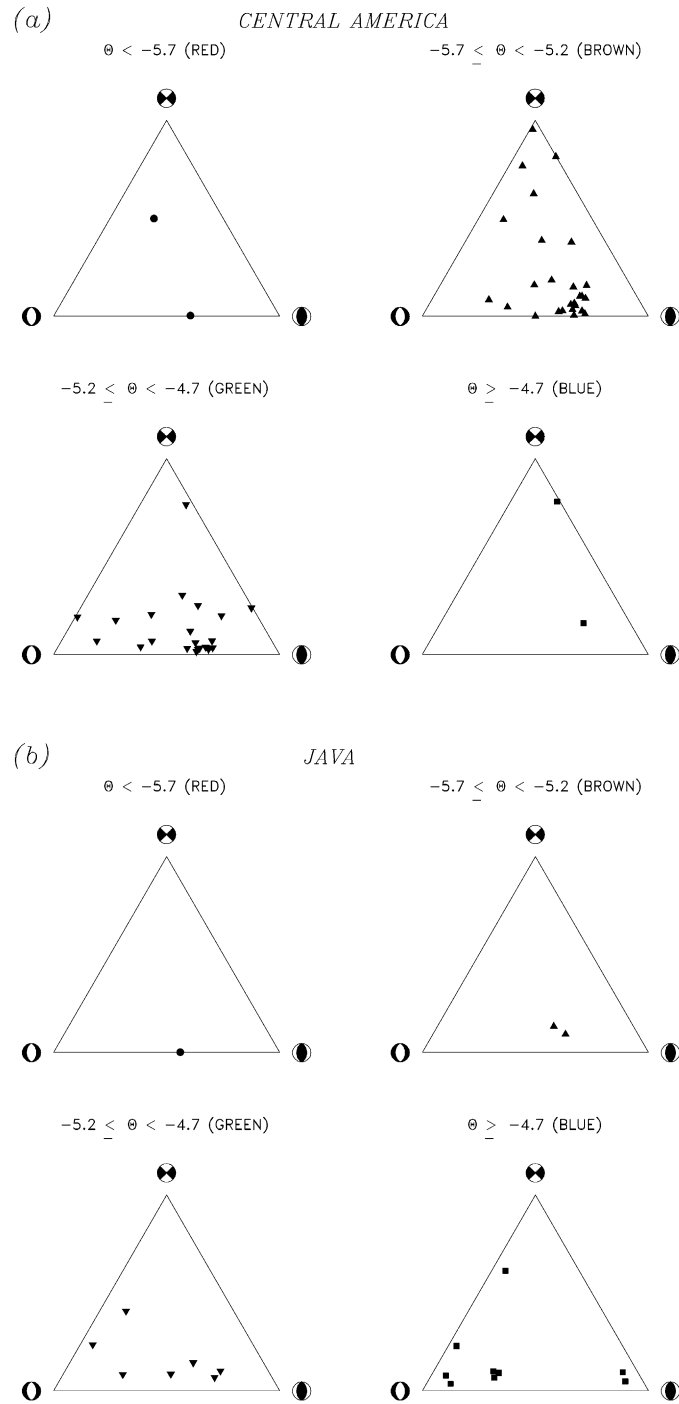


Fig. 6. (a) Central American dataset plotted as a function of focal mechanism, using the formalism of Frohlich and Apperson (1992). The four triangular diagrams correspond to the various subsets color-keyed on Fig. 2 according to their values of the slowness parameter  $\theta$ . (b) Same as (a) for Java. (c) Same as (a) for Peru. Note that in all regions, no correlation is found between slowness and focal mechanism.

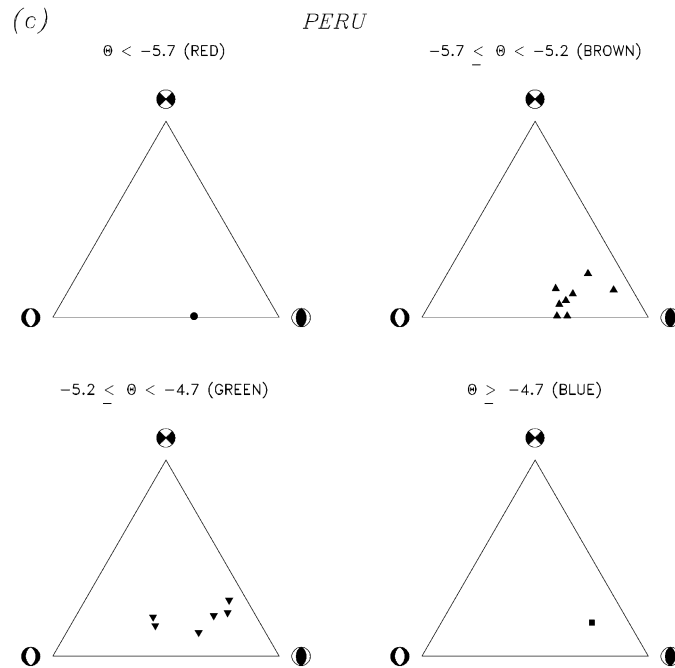


Fig. 6 (Continued).

oriented vertically; this simply expresses the fact the only two earthquakes in the dataset with a strong component of strike-slip are fast (11 March 1982,  $\Theta = -4.39$ ; 17 December 1987,  $\Theta = -4.85$ ); the correlation falls to 0.22 when those two shocks are omitted.

We conclude that source slowness is not correlated with focal mechanism in any of the three regions under study.

### 3.3. Correlation with size

In paper I, we had already rejected any correlation of the Parameter  $\Theta$  with earthquake size. In Fig. 7, we again explore this possibility on each of our regional datasets. The dashed lines are the regressions of each set, once the anomalous tsunami earthquake (shown with a bull's eye symbol) has been removed. Only in Peru do we obtain a significant correlation coefficient (41%), with  $\Theta$  increasing slightly with  $\log_{10} M_0$  (with a slope of 0.19). In the other two areas, the correlation is nonexistent ( $-4$  and  $-7\%$ ). We conclude that the anomalously slow earthquakes (which all have large moments) are not simply the expression of a regional trend in  $\Theta$  as a function of  $M_0$ .

## 4. Regional studies

In this section, we discuss each region individually, and augment its dataset by including selected historical (pre-digital) earthquakes. Results are listed in Table 2 and color-keyed in fainter tones on Figs. 2–4 for the same intervals of the parameter  $\Theta$ . Representative focal mechanisms are used to plot those historical events for which no published mechanism could be found in the literature.

### 4.1. Central America (figures 2 and 8)

We first examine this region, defined as extending from  $99^\circ\text{W}$  (southern Mexico) to  $81^\circ\text{W}$  (Panama), but excluding the Caribbean shore of the isthmus. The average value of  $\Theta$  for the central American digital dataset is  $-5.25$ . Only two earthquakes out of 50 qualify as slow: the 1992 Nicaragua tsunami earthquake, and a small event on 11 March 1988 in Costa Rica. For the 1992 event, we obtain  $\Theta = -6.30 \pm 0.07$ , making it the slowest event in both our present digital dataset and that of Paper I, and confirming its exceptionally slow character, already documented in

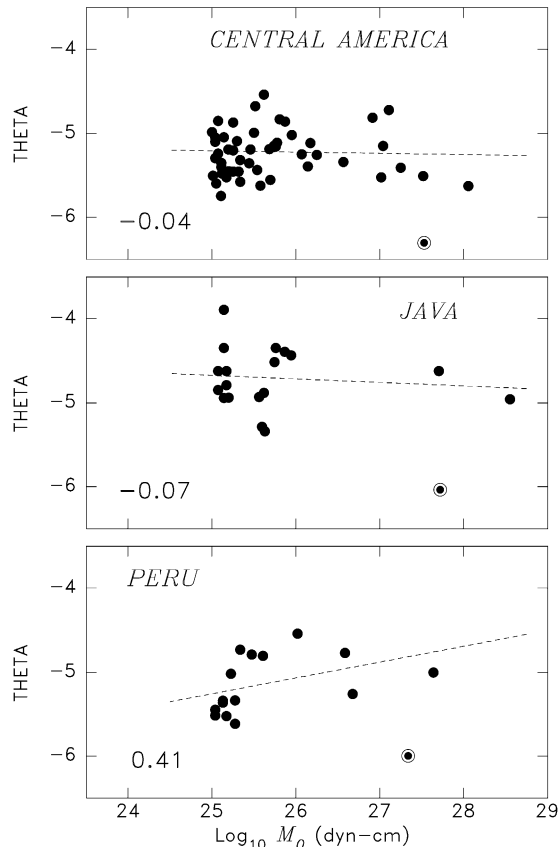


Fig. 7. Values of  $\Theta$  plotted vs. moment for the digital datasets. In each region, the tsunami earthquake is shown with a bull's eye symbol. The best-fitting regressions (with the tsunami earthquakes excluded) are shown as dashed lines, with the correlation coefficients listed at bottom left of each frame.

a number of previous studies (Kikuchi and Kanamori, 1995; Schindelé et al., 1995; Paper I). The 1988 earthquake is marginally slow with significantly greater scatter ( $\Theta = -5.74 \pm 0.31$ ). Both its depth (given as 23 km by both the ISC and NEIC, but 37 km by Harvard) and mostly strike-slip focal mechanism would suggest that, it is not located at the subduction interface, but rather in the overlying wedge.

Fig. 8 shows a close-up of the 1992 epicentral region, including models of the fault zone. Only two aftershocks of the 1992 tsunami earthquake could be analyzed in this study, at 18:28 on the same day (2 September 1992), and at 21:48 on 5 September; neither exhibits slowness ( $\Theta = -5.40$  and  $-5.10$ ,

respectively). Nor do the two earthquakes in our dataset closest to the 1992 epicenter: these are the thrusting event of 19 April 1985, at a distance of 51 km and inside the zone of faulting, and the outer rise normal faulting shock on 15 March 1994, at a distance of 73 km. In this respect, the digital dataset does not suggest that the fault zone of the 1992 earthquake possesses a permanent and systematic propensity to slowness.

We then focus on the other major earthquakes in that subduction zone, and especially the tsunamigenic ones. In Paper I, we had processed the earthquakes of 19 June 1982 off the Guatemala-El Salvador border ( $M_0 = 1.1 \times 10^{27}$  dyn cm;  $\Theta = -5.52$ ) and of 25 March 1990 in Costa Rica ( $M_0 = 1.1 \times 10^{27}$  dyn cm;  $\Theta = -5.15$ ). We confirm that neither of them, nor the Costa Rican event of 3 April 1983 ( $M_0 = 1.8 \times 10^{27}$  dyn cm;  $\Theta = -5.41$ ) is slow; the 1992 earthquake does indeed stand in contrast to other major events in the region. We also include in Table 2 and on Fig. 8 preliminary results obtained for the recent El Salvador earthquake of 13 January 2001 by application of our algorithm at the Pacific Tsunami Warning Center (Weinstein, personal communication, 2001); this event, which shares its intra-slab, normal faulting character with the nearby 1982 earthquake, is fast ( $\Theta = -4.79$  for  $M_0 = 4 \times 10^{27}$  dyn cm); it generated only minor, local tsunami waves.

Next, we turn to historical earthquakes, and first attempt to find large events at the same epicenter as the 1992 tsunami earthquake. There are two large earthquakes reported between  $85.5$  and  $89^\circ$ W, on 29 April 1898 and 28 March 1921, respectively. Relocations of the latter suggest that it was of intermediate depth, thereby explaining the absence of tsunami reports. For lack of data, the former one could not be studied; it is not listed by Solov'ev and Go (1984a), despite a magnitude of 7.9 assigned by Richter. Thus, we cannot address the crucial question of the compared source slownesses of repeat events occurring at the same location along the subduction zone.

We then examine historical events known to have generated destructive tsunamis. In the past 100 years, and for central America east of  $98^\circ$ W, Solov'ev and Go's (1984a) and Solov'ev et al. (1986) monumental compilations list only one tsunami of devastating amplitude, on 26 February 1902, along the coast of Guatemala and El Salvador. This event is particularly

Table 2  
Additional dataset, principally from analog records

Date (D M (J) Y)	Epicenter		Depth (km)	Seismic moment		Estimated energy $E^E$ ( $10^{21}$ erg)	$\Theta$	No. of records	Variance
	$^{\circ}$ N	$^{\circ}$ E		$10^{27}$ dyn cm	Reference <sup>a</sup>				
Central America									
18 July (199) 1934	7.86	−82.40	10	2.1	a	54.	−4.59	1	0.0
5 October (278) 1950	10.35	−85.27	10	2.3	b	67.6	−4.54	2	0.03
19 February (050) 1954 (00:40)	11.78	−86.96	73	0.195	b	0.170	−6.06	1	0.0
19 February (050) 1954 (21:34)	12.10	−86.71	87	0.219	b	0.129	−6.23	1	0.0
24 October (298) 1956	11.79	−86.46	25	0.63	b	2.09	−5.48	1	0.0
24 April (114) 1959 <sup>b</sup>	11.43	−86.41	45	0.01	b	0.006	−6.19	1	0.0
23 August (235) 1978	10.20	−85.22	56	0.33	c	1.86	−5.25	1	0.0
27 May (148) 2000	11.67	−86.98	72	0.004	b	0.02	−5.30	1	0.0
13 January (013) 2001	12.77	−88.83	40	4.0	f	64.5	−4.79	29	
Peru									
5 May (126) 1940	−6.69	−80.41	10	0.15	b	0.166	−5.95	2	0.1
24 May (145) 1940	−11.22	−77.79	10	25.0	d	135.	−5.27	1	0.0
24 August (236) 1942	−14.89	−74.90	10	13.0	d	70.6	−5.26	2	0.03
20 November (325) 1960	−6.72	−80.90	10	2.7	d	2.02	−6.13	1	0.0
29 August (241) 1963	−7.10	−81.60	10	0.22	b	2.74	−4.90	1	0.0
17 October (290) 1966	−12.27	−77.80	38	19.5	e	49.0	−5.60	2	0.10
3 September (246) 1967	−10.59	−79.67	29	0.63	b	38.0	−4.22	1	0.0
30 July (212) 1968	−6.93	−80.46	36	0.096	b	0.054	−6.25	1	0.0
3 October (276) 1974	−12.39	−77.66	9	14.8	b	28.2	−5.72	2	0.10

<sup>a</sup> References for moment estimates: a, Brune and Engen (1969); b,  $M_m$ , this study; c, Dziewonski et al. (1987); d, Okal (1992); e, Abe (1972); f,  $M_m$  (Weinstein, personal communication, 2001).

<sup>b</sup> Tentative value (see text); event shown as triangle on Fig. 8, not shown on Fig. 2.

intriguing, since no earthquake is reported on that day, while major earthquakes took place in the area on 18 January and 19 April of the same year, the latter assigned  $M_{PAS} = 8.3$  by Gutenberg. This scenario, partially reminiscent of the 1932 series off the coast of Colima, Mexico (Sanchez and Farreras, 1993), could suggest either a slow earthquake, undetected in the then poor seismic record, or slumping in the aftermath of the first shock.

The only other major earthquakes having generated tsunamis in the area are the shocks of 5 October 1950 in Costa Rica and 18 July 1934 in western Panama. As discussed in detail in Appendix A, both events are found to be fast, a result upheld by the extensive reported earthquake damage (hence the strong accelerations), and the comparatively minor tsunamis.

Finally, we examine systematically earthquakes pre-dating the digital networks, and with reported locations in the immediate vicinity of the 1992 Nicaraguan earthquake. These include the shocks of 19 February 1954 (two events), 24 October 1956, 24

April 1959, and 19 December 1978. We also include a very recent small earthquake on 27 May 2000, which could share its epicenter with the first 1954 shock, and falls on the boundary of the 1992 fault zone. All details are given in Appendix A. Most of these events exhibit no more than a small trend towards slowness, with  $\Theta$  values in the range  $-5.3$  to  $-5.5$ , but the two 1954 shocks show a strong slowness, with values of  $\Theta$  less than  $-6$ ; note that these events are relatively deep (73–87 km). The 1959 event is also probably slow, this result being tentative on account of an instrumental glitch (see Appendix A). Thus, the 1954 shocks reveal an interesting pattern, namely, that some propensity for slowness may be preserved downwards along the slab to depths of 70–90 km. We note however that neither the recent 2000 event nor earthquakes of comparable depths 50 km to the northeast (18 July 1983; 17 November 1987) exhibit slowness. As for the 1959 event, its immediate three-dimensional neighbors (20 December 1984; 3 April 1990) show no slowness. The slow region may

## NICARAGUA CLOSE-UP

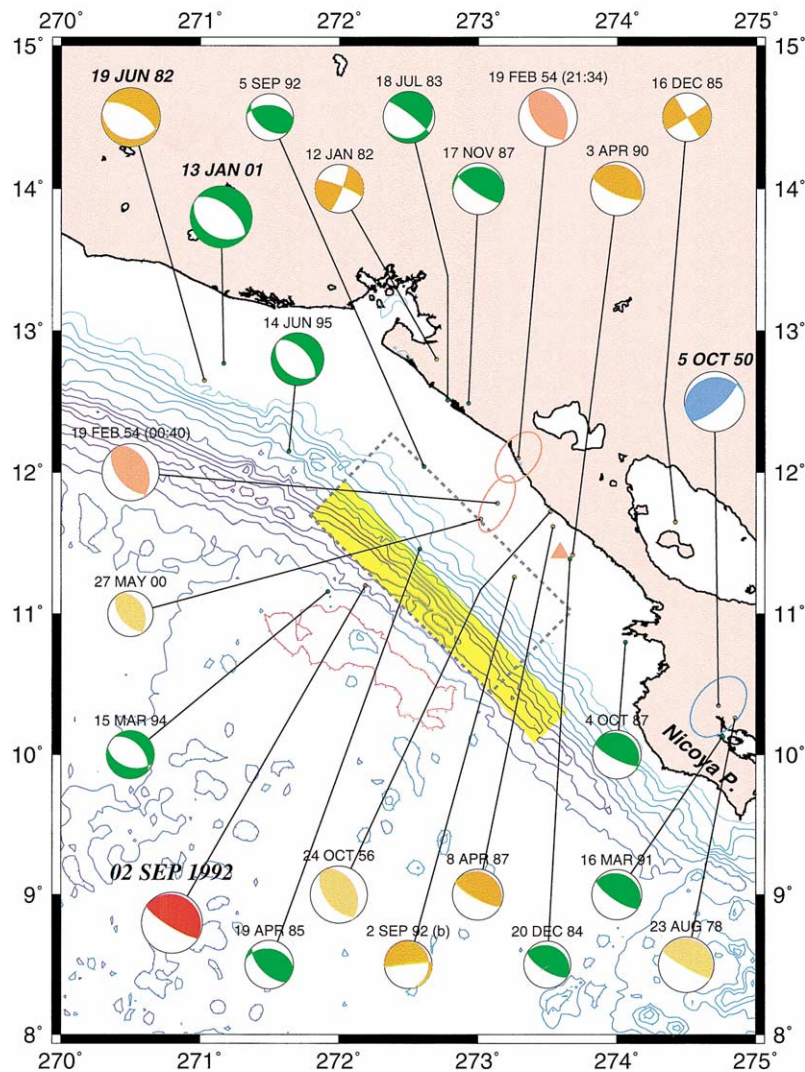


Fig. 8. Close-up of Fig. 2 in the vicinity of the 1992 Nicaraguan event. Bathymetry is at 500-m intervals. Error ellipses are shown for the slow doublet of 19 February 1954. The triangle identifies the epicenter of the 1959 earthquake, which may feature slowness. The dashed box is the rupture area of the earthquake in the seismological model of Satake (1995), while the yellow stripe is preferred by Satake on the basis of tsunami inversion.

thus be more restricted at depth than near the surface, where the 1992 earthquake slow rupture propagated laterally over close to 150 km (Fig. 8).

In seeking a tectonic explanation for the occurrence of slow earthquakes along a narrow segment of the central American subduction system, we first note

that the slow earthquakes occur on a section of slab subducting at a steeper angle under Nicaragua than under Costa Rica, with the slab strongly warped (the so-called ‘Quesada sharp contortion’) at the eastern end of the Nicoya Peninsula (Protti et al., 1995). The angle of subduction reaches  $70^\circ$  in Nicaragua, which

these authors attribute to the greater age of the sea floor in Nicaragua, the Costa Rican portion of the Cocos plate emanating from the propagating Galápagos rift rather than from the east Pacific rise (Hey, 1977). This geometry of the Benioff zone continues westwards to the triple junction at the Mexican–Guatemalan border, beyond which the Cocos plate subducts under North America, at a significantly shallower angle ( $35^\circ$ ). The cause of this change in geometry is unclear since the age of the Cocos plate remains continuous across the junction and the rate of convergence shows only a minor variation, from 6.9 cm per year under the Caribbean plate to 7.7 cm per year under North America (DeMets et al., 1990).

It is remarkable that the steeply dipping segment of subduction zone coincides with a gap in major underthrusting earthquakes. Note in particular that, on the basis of the isoseismal dataset reproduced in Solov'ev and Go (1984a), the epicenter of the large earthquake of 19 April 1902 discussed above must have been close to the Mexican border, and hence the event could have been a Cocos–North America interplate earthquake. As for the large destructive shocks of 1982 and 2001 in El Salvador, they are intra-slab earthquakes, and we therefore conclude that the 1992 tsunami earthquake in Nicaragua took place inside a gap, where no catastrophic ‘megathrust’ interplate earthquakes are known.

In recent reviews of the local framework of subduction based on extensive multichannel seismic reflection surveys, von Huene et al. (2000) and Ranero et al. (2000) pointed out that seafloor topography on the subducting plate changes significantly from a smooth ‘Nicaraguan’ basin west of Fisher ridge (intersecting the trench around  $85.2^\circ\text{W}$ , at the southeastern tip of Nicoya Peninsula) to a ‘Costa Rican’ province to the east, heavily populated with seamounts and the Cocos ridge. Such structural differences confirm the “rough/smooth boundary” defined by Hey (1977), and may alter the regime of subduction, and in particular, the influx of sedimentary material. However, they predict a smoother fabric on the Nicaraguan side, which would not produce the roughness required in the model of Tanioka et al. (1997), although such roughness could be present on a much smaller scale.

Significant along-strike variation is also found in the properties of central American volcanoes, most evident among them being the lateral offset, about 50 km inland, of the Nicaraguan volcanoes with

respect to Costa Rica, and to a lesser extent, El Salvador. In addition, the Nicaraguan lavas are characterized by strong anomalies in trace element composition and isotopic ratios: they feature enhanced values of Ba/La, Ba/Th, U/Th, B/La, depleted values of Ce/Pb, and higher  $^{10}\text{Be}/^9\text{Be}$  and  $^6\text{Li}/^7\text{Li}$ , as compared to neighboring lavas from Costa Rica and El Salvador (Morris et al., 1990; Chan et al., 1999; Patino et al., 2000). In this context, we note that the 1992 tsunami earthquake (and the slow 1954 events at greater depth) occurred precisely along the segment involving steeper subduction and singular trace element and isotopic ratios. Because we deal with a single tsunami earthquake, the coincidence may be fortuitous, but it remains remarkable. Although no definitive model is available for the lateral variations in trace element composition and geochemistry, they are generally assumed to express a larger contribution from slab fluids in Nicaragua. On the other hand, Ranero et al. (2000) find no morphological evidence for a difference in flux of sedimentary input along the Nicaraguan segment of the subduction system, suggesting that the greater fluids contribution is controlled by thermodynamic parameters rather than directly by the volume of subducted sediments. Whether or not these parameters could also control the nature of rupture on the 1992 fault plane (and on the deeper 1954 ones) remains speculative.

In conclusion of this regional study, the slow source characteristics of the 1992 Nicaragua earthquake are not shared by the overwhelming majority of the events investigated. In particular, they are not found in any of the other large earthquakes at the central American subduction zone, even though several raised significant tsunamis. These events took place along other segments of the subduction zone, featuring different subduction characteristics in terms of geometry, lithospheric age, and arc volcanism. While this points to a highly localized source of earthquake slowness, constrained to the 200 km stretch of Nicaraguan coastline, we note that the 1992 aftershocks, and several events occurring independently inside the 1992 fault zone, do not exhibit slowness. This could be explained by Tanioka et al. (1997), in which slowness results from jerky rupture across a highly fragmented slab–mantle interface, and is thus absent from smaller events involving a source region of lesser dimensions. In turn, the fragmentation could be due to enhanced flexure

of the plate as it subducts at a steeper angle. We note the presence of a bathymetric bulge (red isobath on Fig. 8) on the outer rise of the Cocos plate, across from the 1992 fault zone; we can only speculate as to whether this bulge could sustain a large normal faulting event of a geometry comparable to the 1933 Sanriku earthquake (Kanamori, 1971), which generated the deadliest tsunami of the 20th century. There remains the intriguing observation of the deeper 1954 slow earthquakes, whose origin may be linked to the dehydration of subducted phases. Thus, it is possible that different mechanisms may be responsible for the slow earthquakes of 1992 and 1954.

#### 4.2. Java (figures 3 and 9)

We define this region as extending from the Sunda straits at 105°E to the Australian collision zone at 121°E. We also include for reference the 1992 Flores event in the back arc. The average  $\Theta$  for the whole digital dataset of 19 events is noticeably high:  $\Theta_{av} = -4.78$ , with the 1994 tsunami earthquake clearly its only slow member. The other two large earthquakes studied, the 1977 Sumbawa and 1992 Flores events, feature regular values of  $\Theta$  ( $-4.95$  and  $-4.62$ , respectively). The former was studied by Silver and Jordan (1983), who determined an essentially flat source spectrum for a shallow centroid. The latter, which took place on the back side of the Sunda arc, generated a destructive tsunami; however, several previous studies have established that its source spectrum was not anomalous (Hidayat et al., 1995; Schindel e et al., 1995). The locally catastrophic run-up heights of its tsunami were concentrated along very short segments of coastline, and are generally interpreted as the result of localized underwater landslides triggered by the strong accelerations of the earthquake (Imamura et al., 1995). Our study confirms that the Flores earthquake does not qualify as a ‘tsunami earthquake’.

We were able to analyze five aftershocks of the 1994 Java ‘tsunami earthquake’. Remarkably, and as discussed by Felzer et al. (1999) and Polet and Kanamori (2000), all of them have normal faulting mechanisms, suggesting that they must have taken place on different fault systems. At any rate, all of them exhibit a very fast source.

Regarding historical tsunamigenic earthquakes along the Java–Sumba part of the Sunda arc, their

record is meager. This is due primarily to the weakly coupled character of the subduction, which involves old lithosphere, and a very steep dip of the Benioff zone (Uyeda and Kanamori, 1979; Ruff and Kanamori, 1980). As a result, the largest reverse faulting solution in the CMT catalogue (exclusive of the 1994 event) has a moment of less than  $10^{26}$  dyn cm. Among pre-digital events, we know of no major earthquake with a computed seismic moment. The earthquake with the largest reported magnitude in the area is the shock of 27 February 1903 in the Sunda Straits ( $M_{PAS} = 8.1$ ), but there is no record in the monograph of Solov’ev and Go (1984b) of any tsunami following this event. The next largest event occurred on 11 September 1921 ( $M_{PAS} = 7\frac{1}{2}$ ). Using the technique of Wyssession et al. (1991), we relocate it at 10.98°S; 111.45°E, 175 km west of the 1994 tsunami earthquake. This epicenter is remarkably well constrained for such an old event, with the Monte Carlo ellipse ( $\sigma_G = 10$  s) extending only  $\pm 150$  km in the northeast direction, and excluding the 1994 epicenter (Fig. 3). In complete contrast to the 1994 earthquake, the 1921 event was felt over a very wide area, from Sumatra to Sumbawa, but raised a tsunami of only 10 cm in maximum amplitude. This suggests that its source was not slow.

The only other shock of non-volcanic origin to have generated tsunami waves reaching 1 m (at Butung, south of Sulawesi) took place on 7 January 1925 (Visser, 1926), but the earthquake was reported felt only on Bali, Lombok, and the easternmost coast of Java, some 800 km away, and is absent from worldwide catalogues (NEIC, ISS, BCIS); this intriguing situation might suggest a slow earthquake, but could not be further investigated; at any rate, the reported tsunami remained moderate, and involved the Flores Sea in the back of the arc.

Finally, we were unable to obtain adequate records of historical earthquakes of sufficient size located in the immediate vicinity of the 1994 tsunami earthquake.

We conclude this regional study by stressing the uniqueness of the 1994 tsunami earthquake: it is clearly unique in terms of its slowness, and it is also the only thrust faulting earthquake in 100 years to have generated a lethal tsunami on the southern (ocean) side of the Sunda arc. The catastrophic tsunami, which killed 250 people, is a probable combination of the large low-frequency moment of the seismic source,

and of the significant horizontal displacement incurred by the ocean floor during the rupture (Tanioka and Satake, 1996). We note that the 1994 Java earthquake occurred in a transitional region, where the crust of the overlying Eurasian plate evolves from a thick ‘continental’ character under Sumatra and west Java, to a thinner, more ‘oceanic’, one under Bali (Hamilton, 1979; Gasparon and Varne, 1998). Even though the morphology of the Wadati–Benioff zone (both its dip angle and the distribution of seismicity with depth) shows no significant heterogeneity in east Java (Kirby et al., 1996), the change of overlying crustal structure may locally affect the flexure of the subducting plate, and result in the horst-and-graben system advocated by Tanioka et al. (1997). Finally, we could not correlate

the epicentral area with any clear pattern in the trace element and geochemical characteristics of the arc volcanoes of Java and Bali; we note however, the intriguing presence of the complex Ringgit–Beser volcanic structure in easternmost Java, aligned perpendicular to the trench with the 1994 epicenter (star on Fig. 9), and featuring atypical potassic alkaline lavas, suggestive of a high degree of local heterogeneity in the mantle wedge under east Java (Edwards et al., 1994).

#### 4.3. Peru (figures 4 and 10)

Our study area in Peru is bounded by latitudes  $5^{\circ}\text{S}$  and  $18^{\circ}\text{S}$ . Once again, the 1996 Chimbote ‘tsunami earthquake’ is the only event exhibiting slowness

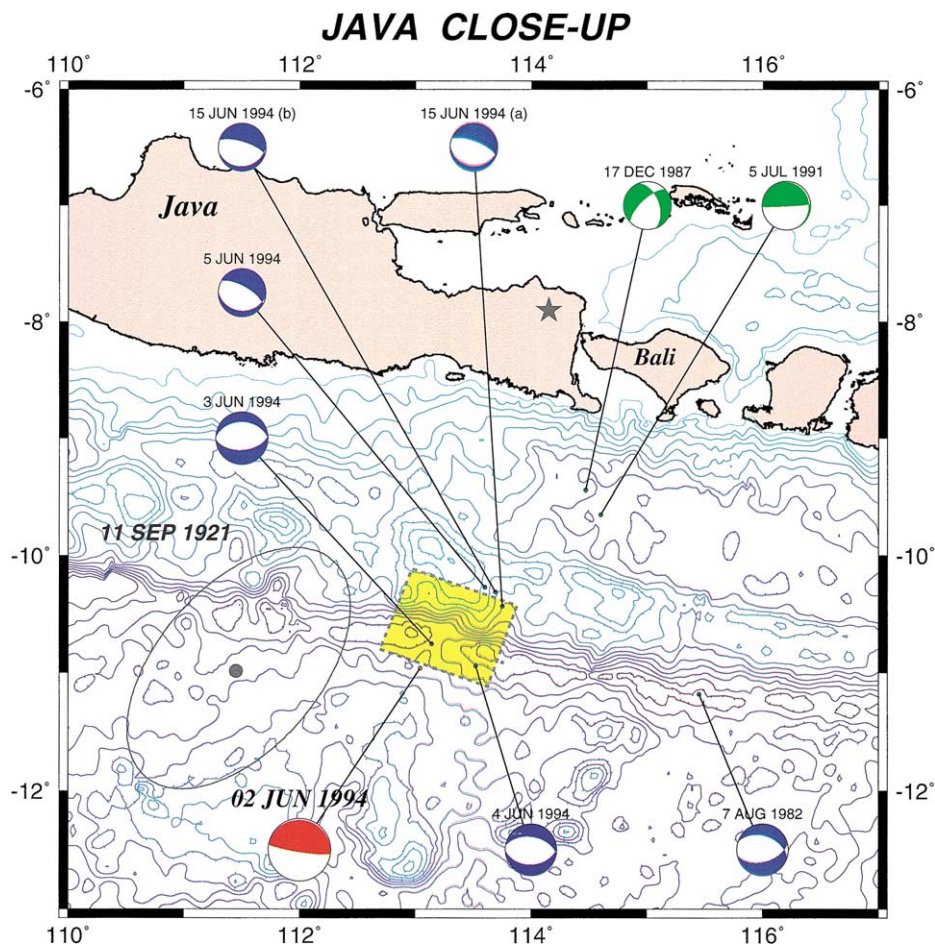


Fig. 9. Same as figure 8 for Java. The rupture area is after Tanioka and Satake (1996). The star identifies the location of the Ringgit–Beser volcanic complex in eastern Java.

in our digital dataset of 15 earthquakes. The comparison is particularly interesting with a large earthquake a few months later along the Nazca coast (12 November 1996), the latter having a standard source time behavior ( $\Theta = -5.00$ ). The average value of  $\Theta$  in the region is  $-5.19$ , and only one earthquake, far inland in the South American continent, features a fast mechanism (19 November 1982;  $\Theta = -4.54$ ). No aftershocks of the Chimbote earthquake were of sufficient size to be processed.

The record of pre-digital tsunamigenic events in Peru is much richer than in the other two regions. Of direct interest to the present study is the tsunami earthquake of 20 November 1960, whose slow character was noted by Abe (1979) and Pelayo and Wiens (1990). Using a Benioff 1–60 record at Weston, we determined an estimated energy of only  $2.0 \times 10^{21}$  erg, which, combined with Okal's (1992) moment estimate of  $2.7 \times 10^{27}$  dyn cm, leads to  $\Theta = -6.13$ ; note that Pelayo and Wiens' moment estimate is slightly larger, which would make the earthquake even slower. Our study confirms that this event is undoubtedly slow, and we show it in pink on Figs. 4 and 10. Thus, this region has at least two documented cases of tsunami earthquakes over the past 40 years.

Next, we investigate systematically the great earthquakes, most of them tsunamigenic, which occurred along the Peruvian coast, as described by Beck and Ruff (1989) and Beck and Nishenko (1990), who quantified their moments at low frequency. This includes the events of 24 May 1940, 24 August 1942, 17 October 1966, 3 September 1967, and 3 October 1974. In addition, we examine earthquakes located in the immediate vicinity of the slow events of 1996 and 1960. For the former, we could find only earthquakes too small for study (no magnitude reported larger than 5.2). Around the 1960 epicenter, we identified and processed three events, on 5 May 1940, 29 August 1963, and 30 July 1968. We refer to Appendix A for all details of this investigation.

Several fundamental results are evident from Figs. 4 and 10. First, this region is unique in our study in featuring two tsunami earthquakes (1960 and 1996) in separate areas, about 400 km apart. In contrast, the other large tsunamigenic earthquakes taking place along the Peruvian coast do not exhibit an anomalously slow regime of moment release. These include the large historical events of 1940, 1942 and 1966,

and the Nazca earthquake of 1996. The 1967 event off the coast of Ancash is even remarkably fast. The case of the Lima earthquake of 3 October 1974 is singular. It qualifies, albeit marginally, as slow ( $\Theta = -5.72$ ), which is generally supported by Hartzell and Langer's (1993) investigation favoring a source lasting as much as 70 s, with a rupture velocity of at most 2.5 km/s.

The 1996 Chimbote earthquake occurred at the southeastern end of a segment of subduction zone characterized by an essentially flat slab (Barazangi and Isacks, 1976), where 100-km deep hypocenters extend 500 km inland, and arc volcanism is absent. This is a probable consequence of the younger age of the oceanic plate north of the Mendaña fracture zone, and of the high convergence rate. This geometry would then suggest a high level of coupling at the subduction interface (Uyeda and Kanamori, 1979), but the region is in fact a gap in major interplate seismicity, extending along the entire subduction zone from the Carnegie ridge at 2°S to the Mendaña fracture zone at 10.5°S. In particular, Dorbath et al. (1990) have documented that the most recent destructive earthquake in the gap goes back to 1619, and speculated that it could have been a normal faulting event similar to the 1970 intraplate earthquake (Abe, 1972).

In this general framework, the occurrence and slow character of the 1996 Chimbote earthquake are probably controlled by structures on a smaller scale. It is remarkable that this event took place at the locus of subduction of the Mendaña fracture zone under the South American plate (Fig. 10). This feature has been proposed by Hilde and Warsi (1982) as the site of localized spreading, propagating inwards into the Nazca plate, an interpretation confirmed by Huchon and Bourgois (1990) on the basis of a detailed multidisciplinary survey on board N/O Jean Charcot. It is possible that this system perturbs the morphological fabric on the subducting plate, setting the stage for the kind of jerky upwards rupture favored by Polet and Kanamori (2000).

In the case of the northern (1960) tsunami earthquake, our results indicate a zone of potentially systematic earthquake source slowness extending eastwards from the 1960 epicenter (Fig. 10). The depth of the 1960 event is poorly constrained between the surface and 25 km (Pelayo and Wiens, 1990), while that of the 1968 event to the east is well constrained by the ISC at  $36 \pm 6$  km, which may be representative

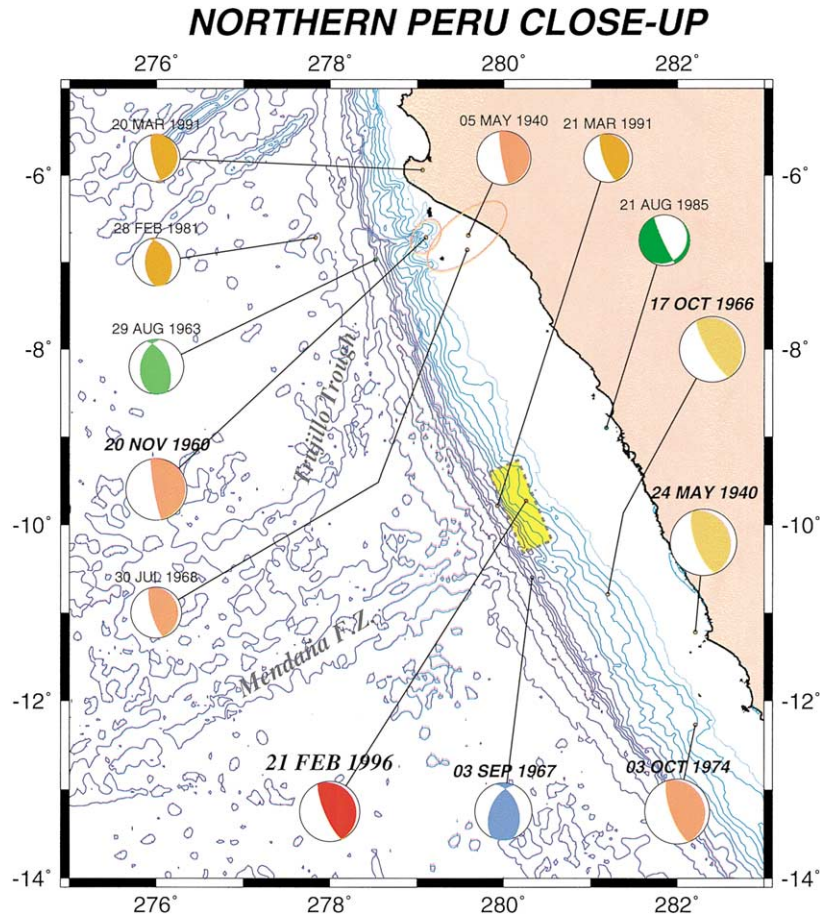


Fig. 10. Same as figure 8 for Peru, showing the Mendaña fracture zone and Trujillo trough (Huchon and Bourgois, 1990). The rupture area is after Ihmlé et al. (1998).

of the top of the slab (Hasegawa and Sacks, 1981). The depth of the 1940 event is unconstrained. Thus, it is possible that slowness is a consistent characteristic of the slab interface in the area. Note that the 1940 and 1968 earthquakes are small ( $M_0 = 1.5 \times 10^{26}$  and  $4.2 \times 10^{25}$  dyn cm, respectively), and thus their rupture would probably not reach into the shallowest portion of the interface, where slow rupture takes place in the model of Tanioka et al. (1997).

The epicentral area of the 1960 shock is one of very complex seafloor morphology and tectonics, the Huancabamba deflection zone (Prince and Kulm, 1975), where the continental slope features numerous deep canyons in the immediate vicinity of the epicenter, and which coincides with the locus of subduction

of the Trujillo trough, a 270-km long feature extending to the small Viru fracture zone, at  $9.5^\circ\text{S}$ ,  $82^\circ\text{W}$ , and which Huchon and Bourgois (1990) have recognized as the site of both transpression and left-lateral strike-slip, possibly related to the opening of the Mendaña fracture zone to the south. Thus, both Peruvian tsunami earthquakes can be correlated with exceptional features strongly perturbing the morphological fabric of the subducting lithosphere.

## 5. Discussion and conclusion

Our study shows that source slowness in tsunami earthquakes cannot be explained by a regional signal

identifiable in other moderate to major events along the same subduction systems, as evidenced by our documentation of only one other slow earthquake (a small strike-slip event in the mantle wedge of Panama) among the 84 shocks comprising our digital dataset. On the other hand, we do find one common denominator to all three recent tsunami earthquakes, namely, that they occur in gaps of major interplate seismic activity — with the possible exception of the 1921 earthquake in Java, of which we know very little, except that it was probably not a tsunami earthquake.

This is generally reminiscent of the observation by Tanioka et al. (1997) along the Sanriku coast, that the tsunami earthquake of 15 June 1896 had occurred along a small segment of subduction zone (their so-called ‘region B’), where large ‘megathrust’ earthquakes are absent (Kawakatsu and Seno, 1983). The extent of that gap is however much larger in Nicaragua and Peru (at least 400 km) than in Sanriku (at most 100 km).

On the other hand, the factors controlling the existence of the gaps must differ in our three study areas: aseismic subduction is easily explained in Java, where the steep dip angle is a consequence of the subduction of Early Cretaceous oceanic lithosphere. In Nicaragua, it is a direct consequence of a local steepening of the subduction, but the latter is not readily explained by the age of the plate which remains relatively young (28 Ma as opposed to 20 in neighboring Costa Rica). As for Peru, the aseismic segment actually corresponds to a younger section of oceanic lithosphere, subducting under South America at an essentially null dip.

When available for study, aftershocks of slow earthquakes do not themselves exhibit slowness. In Nicaragua, this observation leads to the conclusion that the earthquake must grow to a critical minimal size on the fault before it can develop slowness. This would be in general agreement with models in which slowness develops by the jerky propagation of rupture through horst-and-graben structures in the shallowest portions of the fault plane (Tanioka et al., 1997). In Java, the situation is more complex, since the focal mechanisms of the aftershocks differ from that of the main shock, meaning that they occurred on different fault systems. In Peru, we have no information on aftershocks.

Parameters controlling the precise location of the slow earthquakes on the ‘aseismic’ segments are unclear, especially in view of their low numbers for which a reported coincidence between observations may be fortuitous rather than the result of a true physical correlation. Notwithstanding this caveat, the most remarkable situation is in Peru, where both tsunami earthquakes took place at the sites of subduction of major tectonic features on the Nazca plate, the Mendaña fracture zone under Chimbote and the Trujillo trough to the north, both of which involve significant localized intraplate deformation (Huchon and Bourgois, 1990), and lead to a disruption of the morphology of the subducted seafloor, of the kind required by Tanioka et al. (1997). However, if roughness is present in Nicaragua, it cannot be readily explained from the local tectonic model, which would predict a smoother fabric than in neighboring Costa Rica. Furthermore, such models also require sediment starvation to allow propagation of the rupture upwards into the shallowest part of the fault plane; yet, it has been noted in both Nicaragua (Ranero et al., 2000) and Peru (Moore and Taylor, 1988) that the sedimentary fluxes into the relevant segments of trench are not deficient, at least on a regional scale (in Peru, there remains the possibility that those fluxes could be locally affected by the presence of the Mendaña and Trujillo heterogeneities).

In conclusion, we have documented, in the instrumental record, the occurrence of several slow events in areas adjacent or close to the recent tsunami earthquakes in Nicaragua and Peru, but any correlation with definitive spatial parameters remains at this point highly speculative. It is clear that further study of more cases of source slowness in subduction earthquakes is warranted before our understanding of tsunami earthquakes becomes sufficiently well anchored as to give these disasters some level of predictability.

### Acknowledgements

We thank Alan Brandon for enlightening discussions on trace elements and isotopes, Hiroo Kanamori and Don Helmberger for access to the Caltech archives, and Brian Mitchell and John Ebel for providing copies of historical seismograms. Stuart

Weinstein forwarded an early estimate of  $\Theta$  for the 2001 El Salvador earthquake. The paper was improved by insightful comments from two anonymous reviewers. Maps were drawn using the GMT software (Wessel and Smith, 1991).

## Appendix A. Discussion of individual events

We present here a discussion of individual events, mostly from the pre-digital era, studied in the context of the three modern ‘tsunami earthquakes’. In each region, events are listed chronologically. All relocations were carried out using the method of Wyssession et al. (1991), based on ISS or ISC bulletin arrivals.

### A.1. Central America

- 28 March 1921, *Nicaragua*;  $M_{\text{PAS}} = 7.3$ ; no tsunami reported

At  $12.5^\circ\text{N}$ ,  $87.5^\circ\text{W}$ , this event is the largest reported at a longitude comparable to that of the 1992 tsunami earthquake. Relocation efforts converge on  $12.96^\circ\text{N}$ ;  $86.96^\circ\text{W}$ , at the intermediate depth of 143 km, although the Monte Carlo depths ( $\sigma_G = 7$  s) range from 0 to 280 km.

- 18 July 1934, *Panama*;  $M_{\text{PAS}} = 7.7$ ; minor tsunami

This earthquake relocates at  $7.86^\circ\text{N}$ ,  $82.40^\circ\text{W}$ , off the western shore of Panama. Its Monte Carlo ellipse ( $\sigma_G = 5$  s) encompasses three recent earthquakes. The focal mechanism shown on Fig. 2 is from Wickens and Hodgson (1967). For this event, Brune and Engen (1969) report a spectral amplitude measurement of Love waves at 100 s equivalent to a moment of  $2.1 \times 10^{27}$  dyn cm. We obtained a record of this earthquake on the prototype Benioff broadband instrument, which at that time operated at Pasadena with a galvanometer period  $T_g = 70$  s. The absolute gain of the instrument is unreported, but can be calibrated against the result of Brune and Engen (1969) by a mantle magnitude measurement. This suggests a maximum gain of 1500 at 1 s, a legitimate value during the development stages of Benioff’s broadband instrument. When, in turn, this magnification is applied to the energy estimate, we find  $\Theta =$

$-4.59$ , indicating that the earthquake is indeed fast.<sup>2</sup>

- 5 October 1950, *Costa Rica*;  $M_{\text{PAS}} = 7.7$ ; minor tsunami

This earthquake relocates at  $10.35^\circ\text{N}$ ,  $85.27^\circ\text{W}$ , at the northeastern end of the Nicoya Peninsula. This epicenter is shown on Fig. 2 with its associated Monte Carlo ellipse ( $\sigma_G = 4$  s). The focal mechanism shown is after Wickens and Hodgson (1967). Of the Benioff 1–90 Pasadena seismograms, we could process only the  $G_1$  wave, because records were changed during the Rayleigh wave arrival a few minutes later. We obtain a mantle magnitude  $M_m = 7.37$ . We also processed the Love wave recorded on the Wood–Anderson torsion instrument at Florissant, yielding  $M_m = 7.02$ , but this estimate suffers from a lack of calibration of the instrument after 1941. When combined with energy estimates from the two horizontal components of the 1–90 system (the vertical went off scale), we find  $\Theta = -4.51$  (on the NS component) and  $-4.57$  on the EW one. Thus, this earthquake is not slow; the relatively small tsunami generated despite its large moment probably reflects its on-land epicenter.

- 19 February 1954, *Nicaragua*;  $M_{\text{PAS}} = 6.5/8$  (both events); no known tsunami

Two events occurred on that date at 00:40 and 21:34 GMT, respectively. Relocated epicenters are at  $11.78^\circ\text{N}$ ,  $86.96^\circ\text{W}$  (00:40) and  $12.10^\circ\text{N}$ ,  $86.71^\circ\text{W}$  (21:34), the former just 41 km east of the 1992 epicenter. The Monte Carlo ellipses ( $\sigma_G = 3$  s) intersect over a slight area (Fig. 8), but it remains likely that the second shock lies to the northeast of the first one. Floated-depth relocations converge on 73 and 87 km, respectively, while it is probable that the events are indeed deep, Monte Carlo depths range from 16 to 124 km for

<sup>2</sup> Note that the absolute magnification of the instrument does not cancel out of the computation of  $\Theta$  from moment and energy, because the former is linear in ground displacement, the latter in the square of ground velocity. The source of this apparent paradox lies in the fact that an erroneous instrument gain leads to an erroneous value of the moment or ‘size’ of the earthquake, and hence of its source corner frequency, as expected under seismic scaling laws. The latter parameter (or its inverse the rise time  $T_0$  of the source) is necessary for a correct interpretation of the body-wave spectral amplitudes used in the energy calculation as revealing a ‘slow’ or ‘fast’ character of the source; see paper I and Vassiliou and Kanamori (1982) for details.

the first event, and 45 to 130 km for the second one. The second shock is given a focal mechanism ( $\phi = 335^\circ$ ;  $\delta = 39^\circ$ ;  $\lambda = 101^\circ$ ) by Wickens and Hodgson (1967), which we use to plot both shocks on Fig. 8. We processed the vertical Benioff 1–90 records at Pasadena. For both shocks, we find a moment increasing regularly with period ( $M_m = 5.69$  at 54 s, 6.29 at 128 s, and 6.77 at 171 s for the first event;  $M_m = 6.09$  at 54 s, 6.34 at 93 s, and 7.03 at 146 s for the second one). The  $P$ -wave energy is very deficient, leading to  $\Theta = -6.54$  (00:40) and  $-6.92$  (21:34), if the mantle magnitudes at the longest periods are used. These are extremely low values; note however that the use of  $M_m$  computed at intermediate periods (93–128 s) would still define a very slow character for both earthquakes:  $\Theta = -6.06$  (00:40) and  $-6.23$  (21:34); we use these values in Table 2. It is an inescapable conclusion that these earthquakes are indeed very slow.

- 24 October 1956, Nicaragua;  $M_{\text{PAS}} = 7.3$ ; no tsunami reported

This event relocates at  $11.72^\circ\text{N}$ ,  $86.48^\circ\text{W}$ , 93 km east of the 1992 epicenter. We processed the vertical 1–90 record at Pasadena, obtaining  $M_m = 6.80$  at 171 s, and noting a slight increase of moment with period. The body-wave energy leads to  $\Theta = -5.48$ , indicating no more than a slight trend towards slowness. This event is plotted with a representative focal mechanism.

- 24 April 1959, Nicaragua;  $M_{\text{PAS}} = 6.3/8$ ; no tsunami reported

The earthquake relocates at  $11.43^\circ\text{N}$ ,  $86.41^\circ\text{W}$ , 107 km east of the 1992 epicenter. Depth-floated relocations converge on 45 km, but the dataset has little depth resolution, with Monte Carlo depths ( $\sigma_G = 2.5$  s) ranging from 0 to 83 km. It is obviously a much smaller event, and mantle magnitudes processed from the horizontal Press–Ewing records at Pasadena suggest a moment of only  $10^{25}$  dyn cm. The Benioff 1–90 vertical record has a faint  $P$ -wave signal, but is affected by a strong glitch 32 s after the  $P$  arrival. Processing only that short window for  $E^E$  results in a value of  $\Theta = -6.19$ , which would qualify the earthquake as slow, but this result remains tentative given the generally small size of the earthquake. The horizontal 1–90 components only show traces of the  $P$ -wave. We show the event on Fig. 8 as a small triangle. Note that it locates

in the immediate vicinity of four earthquakes with regular source time functions.

- 23 August 1978, Costa Rica;  $M_0 = 3.3 \times 10^{26}$  dyn cm (Harvard CMT)

This event essentially shares its epicenter with the 1950 large shock. No appropriate digital record could be analyzed; the Pasadena Benioff 1–90 vertical yields  $\Theta = -5.25$ , indicative of no source slowness.

- 19 December 1978, Nicaragua;  $M_0 = 5.4 \times 10^{24}$  dyn cm

The epicenter of this event is given by the ISC at  $11.753^\circ\text{N}$ ,  $87.356^\circ\text{W}$ , i.e. less than 2 km from that of the 1992 tsunami earthquake. The only digital record available at an appropriate distance (ZOBO) yields  $\Theta = -5.71$ , bordering on slowness. However, in view of the nodal character of the station, we regard it as inconclusive. The  $P$  wave barely emerges from the noise on the Pasadena 1–90 vertical record, and could not be meaningfully processed for  $E^E$ . In short, with a CMT moment of only  $5.4 \times 10^{24}$  dyn cm, the event is simply too small for the present study.

- 27 May 2000, Nicaragua;  $m_b = 5.0$

This small event occurred essentially at the same location as the first shock (00:40) on 19 February 1954, and at a comparable depth (72 km). We processed broad-band and long-period records at stations FFC and ESK, obtaining the estimates  $M_m = 4.65$  and  $\Theta = -5.37$ . Thus, the event has at best a weak trend towards slowness, but does not share the character of the 1954 shocks or of the 1992 tsunami earthquake. This event is plotted with a representative focal mechanism.

#### A.Z. Peru

- 5 May 1940, northern Peru;  $M_{\text{PAS}} = 6$ ; no known tsunami

The event relocates at  $6.69^\circ\text{S}$ ,  $80.41^\circ\text{W}$ , 54 km east of the 1960 epicenter. No focal mechanism is available. Floated-depth relocations converge on a surficial focus, but some Monte Carlo hypocenters ( $\sigma_G = 3.5$  s) are as deep as 100 km. The vertical 1–90 record at Pasadena yields a mantle magnitude  $M_m = 6.17$ . Both the 1–90 and SPZ  $P$ -wave records are very weak, suggesting  $\Theta = -5.95$ ; in particular, the former is clearly devoid of high-frequency energy (Fig. 1). The earthquake is definitely slow.

- It is plotted with a representative focal mechanism.
- **24 May 1940, central Peru;  $M_0 = 2.5 \times 10^{28}$  dyn cm; significant tsunami reported**  
Beck and Ruff (1989) use a relocation by Dewey at  $11.22^\circ\text{S}$ ,  $77.79^\circ\text{W}$ , and propose an underthrusting mechanism ( $\phi = 340^\circ$ ;  $\delta = 20^\circ$ ;  $\lambda = 90^\circ$ ). The moment of the earthquake was estimated by Kanamori (1977), and confirmed by Okal (1992). We computed an energy estimate from the EW component of the 1–90 system at Pasadena (the other components being too faint), and obtained  $\Theta = -5.27$  in what amounts to an unfavorable focal geometry. The earthquake is not slow.
  - **24 August 1942, southern Peru;  $M_0 = 1.3 \times 10^{28}$  dyn cm (Okal, 1992); significant tsunami reported**  
We relocate this event at  $14.89^\circ\text{S}$ ,  $74.90^\circ\text{W}$ , about 80 km east of the large Nazca event of 12 November 1996. This epicenter is on land, with the Monte Carlo ellipse ( $\sigma_G = 3.5$  s) not intersecting the coastline. A body-wave focal mechanism was published by Swenson and Beck (1996). The moment was revised downwards to  $1.30 \times 10^{28}$  dyn cm from the estimate of Kanamori (1977) by Okal (1992), based on mantle magnitude measurements, and spectral amplitudes reported by Brune and Engen (1969). We processed the NS and EW components of the 1–90 system at Pasadena, and obtained  $\Theta = -5.29$  (NS) and  $-5.24$  (EW). The earthquake is not slow.
  - **20 November 1960, northern Peru;  $M_0 = 2.7 \times 10^{27}$  dyn cm (Okal, 1992); major tsunami, recorded as far as Japan**  
As described in the main text, this event has long been recognized as a slow ‘tsunami earthquake’. We processed the vertical record at Weston (WES), obtained on a Benioff ‘1–60’ instrument, and obtained  $E^E = 2.02 \times 10^{21}$  erg. When combined with Okal’s (1992) moment estimate, this yields  $\Theta = -6.13$ , clearly confirming the slow character of the event.
  - **29 August 1963, northern Peru;  $m_b = 6.1$ ; no known tsunami**  
The event is well located by the ISC at  $6.97^\circ\text{S}$ ,  $81.48^\circ\text{W}$ , 70 km SW of the 1960 epicenter. Stauder (1975) gives a mechanism ( $\phi = 337^\circ$ ;  $\delta = 54^\circ$ ;  $\lambda = 69^\circ$ ), which violates the very sharp impulsive negative first motion at Pasadena (Fig. 1). We took a mantle magnitude measurement on the vertical

Press–Ewing record at Pasadena ( $M_m = 6.39$  with a moment essentially constant with frequency), and an energy measurement on the vertical 1–90 record, leading to  $\Theta = -4.95$ . The earthquake has a regular source time function.

- **17 October 1966, central Peru;  $M_0 = 1.95 \times 10^{28}$  dyn cm (Abe, 1972); major tsunami reported, with decimetric amplitudes in Japan**  
The focal mechanism ( $\phi = 330^\circ$ ;  $\delta = 12^\circ$ ;  $\lambda = 90^\circ$ ) and moment are given by Abe (1972). We processed the vertical 1–90 record at Pasadena, as well as the short-period WWSSN record at Eskdalemuir (ESK), this station selected for its favorable radiation pattern. We obtain  $\Theta = -5.70$  (PAS) and  $-5.51$  (ESK), i.e. or on the average,  $-5.60$ . The event does not formally qualify as slow, but does exhibit some trend towards slowness.
- **3 September 1967, central Peru;  $M_0 = 6.3 \times 10^{26}$  dyn cm; minor tsunami reported**

This earthquake took place 110 km due south of the 1996 event, and is its closest neighbor of significant magnitude. We built its focal mechanism from personal readings of WWSSN first motions; the resulting solution ( $\phi = 342^\circ$ ;  $\delta = 46^\circ$ ;  $\lambda = 59^\circ$ ) differs substantially from Stauder’s (1975). The analysis of long-period Rayleigh waves at Pasadena and several WWSSN stations then yield an average  $M_m = 6.80$ . We computed the estimated body-wave energy from the NS component of the 1–90 system at Pasadena, and obtained  $\Theta = -4.22$ . The earthquake is definitely fast, as was clear from its vigorous high-frequency *P* waves.

- **30 July 1968, northern Peru;  $m_b = 5.8$ ;  $M_s = 6.4$ ; no known tsunami**

This event is well located by the ISC at  $6.86^\circ\text{S}$ ,  $80.42^\circ\text{W}$ , 55 km east of the 1960 epicenter, with a hypocentral depth well constrained at 36 km. Stauder (1975) gives an underthrusting mechanism ( $\phi = 347^\circ$ ;  $\delta = 15^\circ$ ;  $\lambda = 93^\circ$ ). We computed mantle magnitudes from the vertical and EW components of the Press–Ewing records at Pasadena, and obtained  $M_m = 5.55$  ( $G_1$ ) and  $5.70$  ( $R_1$ ), suggesting a moment of  $4.2 \times 10^{25}$  dyn cm. The vertical 1–90 record at Pasadena is remarkably poor in high-frequency energy. Our energy estimate leads to  $\Theta = -5.88$ , which characterizes the earthquake as slow, as could be expected from its significant  $m_b$ : $M_s$  disparity.

- 3 October 1974, central Peru;  $M_0 = 1.5 \times 10^{28}$  dyn cm (Okal, 1992); significant tsunami with decimetric amplitudes in Japan

This large earthquake occurred off the coast of Lima in central Peru. The moment was obtained from Okal and Talandier's (1989) original dataset of mantle magnitudes. The focal mechanism ( $\phi = 340^\circ$ ;  $\delta = 17^\circ$ ;  $\lambda = 90^\circ$ ) is shallow-dipping underthrusting (Beck and Ruff, 1989). We processed the Pasadena vertical 1–90 record ( $\Theta = -5.63$ ), as well as a short-period WWSSN record at Windhoek (WIN), this station being selected for its more favorable radiation pattern ( $\Theta = -5.84$ ). The average value ( $\Theta = -5.72$ ) characterizes the event as marginally slow.

## References

- Abe, K., 1972. Mechanisms and tectonic implications of the 1966 and 1970 Peru earthquakes. *Phys. Earth Planet. Int.* 5, 367–379.
- Abe, K., 1979. Size of great earthquakes of 1837–1974 inferred from tsunami data. *J. Geophys. Res.* 84, 1561–1568.
- Barazangi, M., Isacks, B.L., 1976. Spatial distribution of earthquakes and subduction of the Nazca plate beneath South America. *Geology* 4, 686–692.
- Beck, S.L., Nishenko, S., 1990. Variation in the mode of great earthquake rupture along the central Peru subduction zone. *Geophys. Res. Lett.* 17, 1969–1972.
- Beck, S.L., Ruff, L.J., 1989. Great earthquakes and subduction along the Peru trench. *Phys. Earth Planet. Int.* 57, 199–224.
- Benioff, H., 1955. Earthquake seismographs and associated instruments. *Adv. Geophys.* 2, 219–275.
- Boatwright, J., Choy, G.L., 1986. Teleseismic estimates of the energy radiated by shallow earthquakes. *J. Geophys. Res.* 91, 2095–2112.
- Brune, J.N., Engen, G.R., 1969. Excitation of mantle Love waves and definition of mantle wave magnitude. *Bull. Seismol. Soc. Am.* 59, 923–933.
- Byrne, D.E., Davis, D.M., Sykes, L.R., 1988. Loci and maximum size of thrust earthquakes and the mechanisms of the shallow region of subduction zones. *Tectonics* 7, 833–857.
- Chan, L.H., Leeman, W.P., You, C.-F., 1999. Lithium isotopic composition of central American volcanic arc lavas: implications for modification of sub-arc mantle by slab-derived fluids. *Chem. Geol.* 160, 255–280.
- DeMets, D.C., Gordon, R.G., Argus, D.F., Stein, S., 1990. Current plate motions. *Geophys. J. Int.* 101, 425–478.
- Dorbath, L., Cisternas, A., Dorbath, C., 1990. Assessment of the size of large and great historical earthquakes in Peru. *Bull. Seismol. Soc. Am.* 80, 561–576.
- Dziewonski, A.M., Ekström, G., Franzen, J.E., Woodhouse, J.H., 1987. Global seismicity of 1977; centroid moment tensor solutions for 471 earthquakes. *Phys. Earth Planet. Int.* 45, 11–36.
- Edwards, C.M.H., Menzies, M.A., Thirlwall, M.F., Morris, J.D., Leeman, W.P., Harmon, R.S., 1994. The transition to potassic alkaline volcanism in island arcs: the Ringgit-Beser complex, East Java, Indonesia. *J. Petrol.* 35, 1557–1595.
- Felzer, K., Antolik, M., Abercrombie, R.E., Ekström, G., 1999. Source characteristics of the June 2, 1994 Java tsunamigenic earthquake and aftershocks. *Eos, Trans. Am. Geophys. Un.* 80 (46), F751 (abstract).
- Frohlich, C.F., Apperson, K.D., 1992. Earthquake focal mechanisms, moment tensors, and the consistency of seismic activity near plate boundaries. *Tectonics* 11, 269–296.
- Fryer, G.J., Watts, P., 2000. The 1946 Unimak tsunami: near-source modeling confirms a landslide. *Eos, Trans. Am. Geophys. Un.* 81 (48), F748–F749 (abstract).
- Fukao, Y., 1979. Tsunami earthquake and subduction processes near deep sea trenches. *J. Geophys. Res.* 84, 2303–2314.
- Gasparon, M., Varne, R., 1998. Crustal assimilation versus subducted sediment input in west Sunda arc volcanics: an evaluation. *Miner. Petrol.* 64, 89–117.
- Hamilton, W.B., 1979. Tectonics of the Indonesian region. *US Geol. Surv. Prof. Paper* 1078 345 pp.
- Hartzell, S., Langer's, C., 1993. Importance of model parameterization in finite fault inversions: application to the 1974  $M_w = 8.0$  Peru earthquake. *J. Geophys. Res.* 98, 22123–22134.
- Hasegawa, A., Sacks, I.S., 1981. Subduction of the Nazca plate beneath Peru as determined from seismic observations. *J. Geophys. Res.* 86, 4971–4980.
- Hasegawa, H.S., Kanamori, H., 1987. Source mechanism of the magnitude 7.2 Grand Banks earthquake of November 18, 1929: double-couple or submarine landslide? *Bull. Seismol. Soc. Am.* 77, 1984–2004.
- Hey, R.N., 1977. Tectonic evolution of the Cocos–Nazca spreading center. *Geol. Soc. Am. Bull.* 88, 1404–1420.
- Hidayat, D., Barker, J.S., Satake, K., 1995. Modeling the seismic source and tsunami generation of the December 12, 1992 Flores Island, Indonesia, earthquake. *Pure Appl. Geophys.* 144, 537–554.
- Hilde, T.W.C., Warsi, W.E.K., 1982. Subduction-induced rifting of the Nazca plate along the Mendaña fracture zone. *Eos, Trans. Am. Geophys. Un.* 63, 444 (abstract).
- Huchon, P., Bourgois, J., 1990. Subduction-induced fragmentation of the Nazca plate off Peru: Mendaña fracture zone and Trujillo trough revisited. *J. Geophys. Res.* 95, 8419–8436.
- Ihmlé, P., 1996. Monte Carlo slip inversion in the frequency domain: application to the 1992 Nicaragua slow earthquake. *Geophys. Res. Lett.* 23, 913–916.
- Ihmlé, P., Gomez, J.-M., Heinrich, P., Guibourg, S., 1998. The 1996 Peru tsunamigenic earthquake: broadband source process. *Geophys. Res. Lett.* 25, 1691–1694.
- Imamura, F., Gica, E., Takahashi, T., Shuto, N., 1995. Numerical simulation of the 1992 Flores tsunami: interpretation of tsunami phenomena in northeastern Flores Island and damage at Babi Island. *Pure Appl. Geophys.* 144, 555–568.
- Johnson, J.M., Satake, K., 1997. Estimation of seismic moment and slip distribution of the April 1, 1946, Aleutian tsunami earthquake. *J. Geophys. Res.* 102, 11765–11774.

- Kanamori, H., 1971. Seismological evidence for a lithospheric normal faulting: the Sanriku earthquake of 1933. *Phys. Earth Planet. Int.* 4, 289–300.
- Kanamori, H., 1972. Mechanisms of tsunami earthquakes. *Phys. Earth Planet. Int.* 6, 346–359.
- Kanamori, H., 1977. The energy release in great earthquakes. *J. Geophys. Res.* 82, 2981–2987.
- Kanamori, H., 1985. Non-double-couple seismic source. In: Proceedings of the XXIIIrd General Assembly of the International Association of Seismology and Physics of the Earth's Interior, Tokyo, 1985, p. 425 (abstract).
- Kawakatsu, H., Seno, T., 1983. Triple seismic zone and the regional variation of seismicity along the northern Honshu arc. *J. Geophys. Res.* 88, 4215–4230.
- Kikuchi, M., Kanamori, H., 1995. Source characteristics of the 1992 Nicaragua tsunami earthquake inferred from teleseismic body waves. *Pure Appl. Geophys.* 144, 441–453.
- Kirby, S.H., Stein, S., Okal, E.A., Rubie, D., 1996. Deep earthquakes and metastable mantle phase transformations in subducting oceanic lithosphere. *Rev. Geophys. Space Phys.* 34, 261–306.
- Moore, G., Taylor, B., 1988. Structure of the Peru fore-arc from multichannel seismic-reflection data. *Int. Repts. Ocean Drilling Prog.* 112, 71–76.
- Morris, J.D., Leeman, W.P., Tera, F., 1990. The subducted component in island arc lavas: constraints from Be isotopes and B–Be systematics. *Nature* 344, 31–36.
- Newman, A.V., Okal, E.A., 1998. Teleseismic estimates of radiated seismic energy: the  $E/M_0$  discriminant for tsunami earthquakes. *J. Geophys. Res.* 103, 26885–26898.
- Okal, E.A., 1992. Use of the mantle magnitude  $M_m$  for the reassessment of the seismic moment of historical earthquakes. I. Shallow events. *Pure Appl. Geophys.* 139, 17–57.
- Okal, E.A., 1999. The 1998 Papua New Guinea tsunami: an overview. In: Proceedings of the International Conference on Tsunamis, Paris, 26–28 May 1998. European Community Directorate for Science, Research and Development, Paris, pp. 111–116.
- Okal, E.A., Talandier, J., 1989.  $M_m$ : a variable period mantle magnitude. *J. Geophys. Res.* 94, 4169–4193.
- Patino, L.C., Carr, M.J., Feigenson, M.D., 2000. Local and regional variations in central American arc lavas controlled by variations in subducted sediment input. *Contrib. Miner. Petrol.* 138, 265–283.
- Pelayo, A.M., Wiens, D.A., 1990. The November 20, 1960 Peru tsunami earthquake: source mechanism of a slow event. *Geophys. Res. Lett.* 17, 661–664.
- Pelayo, A.M., Wiens, D.A., 1992. Tsunami earthquakes: slow thrust-faulting events in the accretionary wedge. *J. Geophys. Res.* 97, 15321–15337.
- Polet, Y., Kanamori, H., 2000. Shallow subduction zone earthquakes and their tsunamigenic potential. *Geophys. J. Int.* 142, 684–702.
- Prince, R.A., Kulm, L.D., 1975. Crustal rupture and the initiation of imbricate thrusting in the Peru–Chile trench. *Geol. Soc. Am. Bull.* 86, 1639–1653.
- Protti, M., Güendel, F., McNally, K.C., 1995. Correlation between the age of the subducting Cocos plate and the geometry of the Wadati–Benioff zone under Nicaragua and Costa Rica. *Geol. Soc. Am. Special Paper* 295, 309–326.
- Ranero, C.R., von Huene, R., Fluch, E., Duarte, M., Baca, D., McIntosh, K., 2000. A cross section of the convergent margin of Nicaragua. *Tectonics* 19, 335–357.
- Ruff, L.J., Kanamori, H., 1980. Seismicity and the subduction process. *Phys. Earth Planet. Int.* 23, 240–252.
- Sanchez, A.J.D., Farreras, S.F., 1993. Catálogo de tsunamis (maremotos) en la costa occidental de México. World Data Center for Solid Earth Geophysics, Boulder, 1993. Publ. SE-50, 79 pp.
- Satake, K., 1995. Linear and nonlinear computations of the 1992 Nicaragua earthquake tsunami. *Pure Appl. Geophys.* 144, 455–470.
- Satake, K., Tanioka, Y., 1999. Sources of tsunami and tsunamigenic earthquakes. *Pure Appl. Geophys.* 154, 467–483.
- Schindelé, F., Reymond, D., Gaucher, E., Okal, E.A., 1995. Analysis and automatic processing in near-field of the eight 1992–1994 tsunamigenic earthquakes: improvements in real-time tsunami warning. *Pure Appl. Geophys.* 144, 381–408.
- Silver, P.G., Jordan, T.H., 1983. Total-moment spectra of fourteen large earthquakes. *J. Geophys. Res.* 88, 3273–3293.
- Solov'ev, S.L., Go, Ch.N., 1984a. Catalogue of tsunamis on the eastern shore of the Pacific ocean. *Can. Trans. Fish. Aquat. Sci.* 5078, 285 pp.
- Solov'ev, S.L., Go, Ch.N., 1984b. Catalogue of tsunamis on the western shore of the Pacific ocean. *Can. Trans. Fish. Aquat. Sci.* 5077, 439 pp.
- Solov'ev, S.L., Go, Ch.N., Kim, Kh.S., 1986. Katalog tsunami v tikhom okeane, 1969–1982 gg. Nauka, Moskva, 164 pp., (in Russian).
- Stauder, W., 1975. Subduction of the Nazca plate under Peru as evidenced by focal mechanisms and seismicity. *J. Geophys. Res.* 80, 1053–1064.
- Swenson, J.L., Beck, S.L., 1996. Historical 1942 Ecuador and 1942 Peru subduction earthquakes, and earthquake cycles along Colombia–Ecuador and Peru subduction segments. *Pure Appl. Geophys.* 146, 67–101.
- Synolakis, C.E., Bardet, J.-P., Borrero, J.C., Davies, H.L., Grilli, S., Okal, E.A., Silver, E.A., Sweet, S., Tappin, D.R., Watts, P., 2001. The slump origin of the 1998 Papua New Guinea tsunami. *Proc. R. Soc. London, Ser. A*, in press.
- Talandier, J., Okal, E.A., 1989. An algorithm for automated tsunami warning in French Polynesia, based on mantle magnitudes. *Bull. Seismol. Soc. Am.* 79, 1177–1193.
- Tanioka, Y., Satake, K., 1996. Tsunami generation by horizontal displacement of ocean bottom. *Geophys. Res. Lett.* 23, 861–864.
- Tanioka, Y., Ruff, L.J., Satake, K., 1997. What controls the lateral variation of large earthquake occurrence along the Japan Trench? *Island Arc* 6, 261–266.
- Uyeda, S., Kanamori, H., 1979. Back-arc opening and the mode of subduction. *J. Geophys. Res.* 84, 1049–1061.
- Vassiliou, M.S., Kanamori, H., 1982. The energy release in earthquakes. *Bull. Seismol. Soc. Am.* 72, 371–387.
- Visser, S.W., 1926. Vulkanische verschijnselen en aardbevingen in den Oost-Indischen archipel waargenomen gedurende het jaar 1925. *Natuurkundig Tijdschrift voor Nederlandisch Indie* 86, 214–219.

- von Huene, R., Ranero, C.R., Weinrebe, W., Hinz, K., 2000. Quaternary convergent margin tectonics of Costa Rica, segmentation of the Cocos plate, and central American volcanism. *Tectonics* 19, 314–334.
- Wessel, P., Smith, W.H.F., 1991. Free software helps map and display data. *Eos, Trans. Am. Un.* 72, 441 and 445–446.
- Wickens, A.J., Hodgson, J.H., 1967. Computer re-evaluation of earthquake mechanism solutions. *Pub. Dominion Obs.* 33, 560 pp.
- Wysession, M.E., Okal, E.A., Miller, K.L., 1991. Intraplate seismicity of the Pacific basin, 1913–1988. *Pure Appl. Geophys.* 135, 261–359.